

A Model Consistency-Based Countermeasure to GAN-Based Data Poisoning Attack in Federated Learning

Wei Sun, Bo Gao, *Member, IEEE*, Ke Xiong, *Member, IEEE*, Yuwei Wang
Pingyi Fan, *Senior Member, IEEE*, Khaled Ben Letaief, *Fellow, IEEE*

Abstract—In federated learning (FL), although the original intention of “available but not visible” data is to allay data privacy concerns, it potentially brings new security threats, particularly poisoning attacks that target such “not visible” local data. Intuitively, such data poisoning attacks have great potential in stealthily degrading global FL outcomes, and are expected to be even stealthier if being enhanced by generative models like generative adversarial networks (GANs). However, existing defense methods have not been thoroughly challenged in this regard and generally fail to be aware of a local generation of seemingly legitimate poisoned data. With a growing concern on potentially stealthier attacks, in this paper, a cost-effective defense mechanism named Model Consistency-Based Defense (MCD) is proposed, which offers a comprehensive examination of available local models across multiple feature dimensions, providing an indirect yet effective means of identifying hidden data poisoning attackers. To push the limit of MCD against stealthier attacks, we propose a new GAN-based data poisoning attack model named VagueGAN and an unsupervised variant of it, which can be flexibly deployed to generate seemingly legitimate but noisy poisoned data. The consistency of GAN outputs revealed by VagueGAN helps strengthen MCD to work against stealthier GAN-based attacks as well as other mainstream ones. Extensive experiments on multiple open datasets (MNIST, Fashion-MNIST, CIFAR-10, CIFAR-100, and Mini-Imagenet) indicate that our attack method better balances the trade-off between attack effectiveness and stealthiness with low complexity. More importantly, our defense mechanism is shown to be more competent in identifying a variety of poisoned data, particularly stealthier GAN-poisoned ones.

Index Terms—Federated Learning, Security and Privacy, Generative Adversarial Networks, Data Poisoning

I. INTRODUCTION

Emerging as a promising distributed learning paradigm, federated learning (FL) can be used to collaboratively train a deep learning model at a server based on decentralized datasets privately owned by multiple clients. However, the “available but not visible” nature of training data in FL still leads to security risks. A server usually has to rely on the support of a large number of possibly untrustworthy clients, because it is very likely that some of the clients especially crowdsourced

ones are originally manipulated or hijacked by some attackers. More seriously, the server does not have access to the clients’ private datasets that largely determine the quality of training outcomes, so the local data “not visible” to the server or the resulting local models can easily become the best targets of the attackers [1].

Poisoning attacks are the greatest threats in an FL system. An attacker can falsify either the local data (via data poisoning) or the local models (via model poisoning) of compromised clients to indirectly mislead the global model of a server that is built upon those local data or models. Theoretically, such poisoning attacks can be not only effective in undermining the global model but also undetectable by the server without data access. In comparison with the model poisoning attacks, the data poisoning attacks are generally harder to be detected by the server and thus would be more worth studying from both attack and defense perspectives [2].

However, existing research on stealthy data poisoning in FL remains in its infancy. Existing defense methods have not been really challenged due to lack of data poisoning attacks that can ensure both attack effectiveness and stealthiness [3]–[8]. Existing attack methods, however, focus more on attack effectiveness rather than attack stealthiness, thus inevitably giving rise to noticeable changes in local model distributions that can be readily detected by existing defense methods [3], [9]–[16]. Although the stealthiness of data poisoning attacks in FL has not been previously achieved in the existing work, such “not visible” attacks still show great potential in globally degrading FL outcomes while locally hiding themselves, so we must get fully prepared to defend FL systems against upcoming stealthier attacks.

In this paper, we aim to develop a countermeasure to stealthier data poisoning attacks in FL. We are particularly interested in thwarting the potential of generative adversarial network (GAN) models from achieving stealthier attacks. Targeting GAN-based data poisoning attacks as well as other mainstream ones, we propose a cost-effective defense method that captures the historical characteristics of available local models so as to indirectly identify hidden attackers. To push the limit of our defense method against stealthier attacks, we propose a new GAN-based data poisoning method with enhanced attack stealthiness [17]. Instead of producing near-realistic data of high quality through regular uses of GAN, our attack method turns to reversely leverage the power of GAN to generate vague data with appropriate amounts of poisonous noise. The local models poisoned by such vague data can be made globally damaging, while the vague data can keep the statistical characteristics of their GAN inputs so that the local

W. Sun, B. Gao and K. Xiong are with the Engineering Research Center of Network Management Technology for High Speed Railway of Ministry of Education, School of Computer Science and Technology, and the Collaborative Innovation Center of Railway Traffic Safety, Beijing Jiaotong University, Beijing 100044, China. E-mail: {21120398, bogao, kxiong}@bjtu.edu.cn.

Y. Wang is with the Institute of Computing Technology, Chinese Academy of Sciences, Beijing 100190, China. E-mail: ywwang@ict.ac.cn.

P. Fan is with the Beijing National Research Center for Information Science and Technology, and the Department of Electronic Engineering, Tsinghua University, Beijing 100084, China. E-mail: fpy@tsinghua.edu.cn.

K. Letaief is with the Department of Electrical and Computer Engineering, Hong Kong University of Science and Technology, Hong Kong 999077, China. E-mail: eekhaled@ust.hk.

models poisoned can be seemingly legitimate. In addition, it can be computationally efficient to generate vague data of relatively low quality, rendering data poisoning broadly applicable, even for resource-constrained mobile devices. Fortunately, our attack model reveals the consistency of GAN outputs and thus helps strengthen our defense method to work against stealthier GAN-based attacks as well as other mainstream ones. To more effectively establish a safer and more robust FL system, our contributions are as follows.

- In response to stealthier data poisoning attacks, we propose a cost-effective countermeasure named *Model Consistency Based Defense (MCD)*, which comprehensively reviews available local models, and identifies abnormal clients via two statistical metrics inspired by our findings on the consistency of GAN outputs.
- Before that, we propose an attack method named *VagueGAN*, which is a GAN model specially designed for stealthier data poisoning attacks against FL systems. It generates vague poisoned data that can not only effectively but also unnoticeably attack a global model with all labels/classes involved. *To the best of our knowledge, our MCD is the first countermeasure to such a GAN-based attack emphasizing improved attack stealthiness.*
- We develop guidelines for taking full advantage of VagueGAN to achieve a balanced trade-off between attack effectiveness and stealthiness, which is not readily achievable for existing approaches. Furthermore, we propose an unsupervised variant of VagueGAN, along with flexible deployment options, making it broader applicable.
- We conduct extensive experiments on multiple most-used open datasets: i.e., MNIST, Fashion-MNIST, CIFAR-10, CIFAR-100, and Mini-Imagenet. It is verified that the data poisoning attacks enhanced by our VagueGAN not only better degrade FL outcomes with low efforts but also are generally much less detectable. More importantly, our MCD better identifies a variety of poisoned data, particularly stealthier GAN-poisoned ones.

The remainder of this paper is organized as follows. Related work is discussed in section II. Objectives and assumptions are outlined in section III, where the system model and attack model are defined. Our proposed attack is elaborated in section IV. Our proposed defense is suggested in section V. Performance evaluation is presented in section VI. Finally, our conclusions and future work are summarized in section VII.

II. RELATED WORK

Although data poisoning attacks and their countermeasures in regular deep learning systems have been well studied [18]–[21], the research on those in FL systems is still in its infancy.

To mitigate data poisoning attacks against FL systems, some targeted countermeasures have been found to be useful. Some existing works, e.g., [3], [4], [6], [22]–[26] employ similar two-step statistical approaches, where lower-dimensional local models are obtained in the first step and are statistically analyzed for outlier detection in the second step. Specifically, in [3] and [4], the authors propose to use principal component analysis (PCA) and uniform manifold approximation and projection (UMAP) respectively to reduce the dimensions of all

local models to two-dimensional, to facilitate the identification of any abnormal model distribution. In [22], the authors propose proposed divide-and-conquer (DnC), which computes the distance between the maximum variance direction of all local models and the updated scalar product to identify anomalies. In [23], the authors propose FLDetector, where the server predicts every client’s model updates and flags a client as malicious if there is a multi-round mismatch between the client’s uploaded model updates and its predicted ones. In [24], the authors propose a label-flipping-robust (LFR) algorithm based on cosine similarity temporal analysis, which is applicable to both independent and identically distributed (IID) and non-IID data. In [25], the authors propose CONTRA, which implements a cosine-similarity-based measure for outlier detection. In [6], the authors propose proposed local malicious factor (LoMar), which is based on the kernel density estimation and K-nearest neighbor methods. In [26], the authors propose FedDMC, which achieves clustering-based malicious client detection by applying a binary tree-based noise module to the dimension-reduced model parameters. In addition, some defense methods [27]–[33] detect malicious clients by leveraging additional resources or tools to characterize and identify abnormal local models or datasets. However, none of these defense methods works well if attackers can generate seemingly legitimate poisoned data whose statistical distributions approximate normal ones.

As for data poisoning attacks against FL systems, existing works primarily leverage label flipping techniques to generate poisoned local data through falsifying certain labels of training data. Specifically, in [3], the authors propose a label flipping attack to rearrange the label-sample associations of a local dataset to generate a poisoned dataset. In addition, in [18], the authors propose a GAN model for the first time to extract private features of local data from GAN-generated pseudo data after initializing the GAN by the global model. On this basis, in [14], the authors propose to enhance regular label flipping attacks by their PoisonGAN, an off-the-shelf GAN model only used to enlarge the sizes of local datasets with legitimate pseudo samples by using a discriminator initialized by the global model. In [34], the authors propose a clean-label poisoning attack by adding a perturbation to the gradients of adversarial loss, which only generates poisoned features without falsifying labels. However, these attack methods inevitably give rise to significant changes in the local distributions of training data, which can be readily detected by corresponding defense methods. Consequently, they do not currently represent a significant threat, therefore cannot be used to cultivate a robust defense system.

III. OBJECTIVES AND ASSUMPTIONS

In this section, we describe the objectives and assumptions in an FL system.

A. System Model

We consider an FL system that consists of a server and a set $\mathcal{C} = \{c_1, c_2, \dots, c_N\}$ of N mobile clients. A regular training process of FL is considered. Initially, the server distributes an

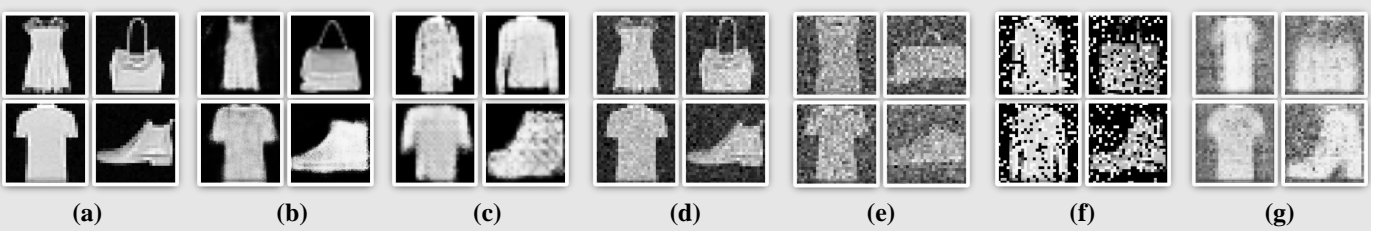


Fig. 1: Comparison of GAN-generated and noise-superimposed samples: (a) Real data; (b) Data generated by regular GAN; (c) Data generated by PoisonGAN for data augmentation only; (d) Data added with light Gaussian noise; (e) Data added with heavy Gaussian noise; (f) Data added with Salt and Pepper noise; (g) Data generated by VagueGAN for direct attack use.

FL main task to each client. In each round $t = 1, 2, \dots, T$ of FL, every client c_i receives model updates from the server and trains a local model $\theta_{t,i}$ on its local dataset \mathcal{D}_i^{train} . To avoid potential network congestions, the server then randomly selects K out of N clients, aggregates their local models into a global model $\tilde{\theta}_t$ and sends it to all the clients for a new round of training. Meanwhile, the server uses a test dataset \mathcal{D}^{test} to obtain the global accuracy a_t of $\tilde{\theta}_t$.

B. Attack Model

a) Attacker's Goal: In an FL system, we assume that there exists at least one data poisoning attacker. The attacker's primary goal is to degrade the performance of the global model as much as possible. Second, the attacker's another equally important goal is to hide its attacks from being detected by the server.

b) Attacker's Capabilities: The attacker is assumed to be capable of carrying out data poisoning attacks. First, the attacker can gain control of one or more benign clients or disguise itself as a benign client. Second, the attacker can gain all the privileges of each controlled client, e.g., local dataset, local model training process, etc.

Due to our focus on data poisoning attacks, the attacker's scope of operation is assumed to be limited to every controlled client. First, we guarantee that the server is completely honest and unattackable. Second, we assume that communication links for FL are reliable and the attacker cannot influence the process of model exchanges over the links. Third, the attacker cannot access any datasets of the server and uncontrolled clients. Finally, the attacker also has no access to the models of uncontrolled clients.

c) Attacker's Approach: The attacker carries out a data poisoning attack to achieve its goals. In particular, the attacker first obtains control of at least one client as malicious client through certain means. Then the attacker poisons the local dataset of the malicious client and obtains a poisoned local dataset using an attack method. Finally, the malicious client trains a poisoned local model on its poisoned local dataset and uploads it to the server. If not being detected by the server, the poisoned local model is expected to harm the global model after model aggregation.

IV. GAN-BASED DATA POISONING ATTACKS

In this section, to push the limit of our defense method against stealthier attacks, we propose a new GAN model called

VagueGAN, which is specifically designed for stealthier data poisoning attacks against FL systems. VagueGAN can help strengthen our defense method to work against GAN-based attacks as well as other mainstream ones.

To this end, subsection IV-A introduces the architecture, loss function, and other design considerations underlying VagueGAN's poisoning ability. Subsection IV-B outlines the overall workflow of a data poisoning attack enabled by VagueGAN. To provide deeper insights, subsection IV-C presents a comprehensive theoretical analysis. Subsection IV-D gives practical guidelines for implementing VagueGAN for a trade-off between attack effectiveness and stealthiness. Finally, subsection IV-E introduces an unsupervised variant of VagueGAN, while subsection IV-F discusses deployment advantages of VagueGAN.

A. VagueGAN Model

A GAN model has a generator G and a discriminator D . On the one hand, the generator G generates fake data samples close to real ones in terms of distribution and tries to convince the discriminator D . On the other hand, the discriminator D tries to distinguish between real and fake samples. They compete with each other in the training phase, thus operating as an adversarial game that makes the generator G outputs approximate original data in distribution.

Our VagueGAN unconventionally leverages the power of GAN to generate seemingly legitimate vague data with appropriate amounts of poisonous noise, in order to achieve a balanced trade-off between attack effectiveness and stealthiness. On the one hand, VagueGAN needs to generate seemingly legitimate poisoned data for a stealthier attack. We extend the Conditional GAN (CGAN) model to generate poisoned data from local data. The architectures of the generator and discriminator of VagueGAN will be optimized in order to achieve superior poisoning results. Similar to the original CGAN, all data is generated through a multi-layer perceptron (MLP)-like network. Beyond the original CGAN, however, three enhancements are put in place for VagueGAN to make resulting poisoned data closer to legitimate ones in their distribution. First, VagueGAN utilizes a much deeper structure in the discriminator (e.g., 4 hidden layers). A deeper discriminator improves attack stealthiness by ensuring that the poisoned data better retains legitimate features even from a small local dataset. Second, VagueGAN also employs techniques such as batch normalization and LeakyReLU to more effectively

capture data features. Third, VagueGAN adopts a large batch size for full dataset training to further obtain the overall features of local dataset.

On the other hand, VagueGAN needs to generate noisy poisoned data for an effective attack, since data noise can easily harm the quality of training data and thus that of resulting trained model. First, besides the discriminator, VagueGAN also utilizes a much deeper structure in the generator (e.g., 4 hidden layers) and techniques such as batch normalization and LeakyReLU. A deeper generator improves attack effectiveness by increasing the uncertainty of data generation and thus making the poisoned data vaguer and noisier. Second, we design a loss function of VagueGAN to break the commonly reached Nash equilibrium by restricting the discriminative ability of the discriminator. This can lower the generation performance of the generator and thus lead to generated data carrying a lot of poisonous noise.

Our loss function is defined as follows:

$$\min_G \max_D V(G, D) = \mathbb{E}_{\mathbf{x} \sim p_d(\mathbf{x})} [\log(1 + \kappa)D(\mathbf{x})] + \mathbb{E}_{\mathbf{z} \sim p_z(\mathbf{z})} [\log(1 - (1 + \kappa)D(G(\mathbf{z})))] \quad (1)$$

where \mathbf{x} is a sample following the original data distribution $p_d(\mathbf{x})$; \mathbf{z} is the sample obtained from a certain distribution $p_z(\mathbf{z})$; $G(\mathbf{z})$ is the fake sample generated by the generator G ; $D(\mathbf{x})$ represents the probability that \mathbf{x} is a real sample. On the one hand, the larger $D(\mathbf{x})$ (or $D(G(\mathbf{z}))$) is, the more accurately the discriminator D can identify original (or generated) samples. Hence, stronger D is obtained to maximize V . On the other hand, if G is stronger, the discriminator will make a misjudgment, and $D(G(\mathbf{z}))$ will become larger. Hence, stronger G is obtained to minimize V . We use a suppression factor $\kappa \in (0, 1)$ to limit the generation ability of the generator G . The larger κ is, the more restrictive it is on the generation ability. Clearly, the value of κ can be used to trade-off the effectiveness and stealthiness of VagueGAN.

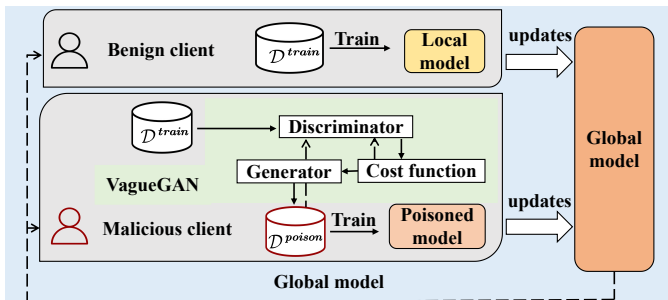


Fig. 2: Use of VagueGAN for a data poisoning attack: A malicious client trains VagueGAN on its dataset to generate an equivalent amount of poisoned data. The poisoned dataset is then used for local training to obtain a poisoned model, which is subsequently uploaded to the server.

To support data poisoning attacks, on the one hand, the generation target of our VagueGAN is much different from that of traditional GANs for regular uses. As shown in Figure 1(b) and 1(g) where taking image data as an example, the sample distribution generated by a traditional GAN is largely fitted to the real sample distribution, but that generated by VagueGAN is just roughly close to the real sample distribution for a balanced trade-off between seemingly legitimate and

noisy results. The samples generated by PoisonGAN (Figure 1(c)) with discriminator D initialized by the global model [14] are also of relatively good quality because PoisonGAN can be considered as a data augmentation method instead of an actual attack method. Furthermore, compared with traditional GANs, our VagueGAN can be more computationally efficient only aiming to generate vague data of relatively low quality. Note that even if being under-trained for data poisoning, traditional GANs usually generate intermediate outputs with certain vagueness but without carrying noise, and thus cannot ensure successful attacks.

On the other hand, the vague data generated by VagueGAN is different from real data superimposed with noise (Figure 1(d), 1(e) and 1(f)). Adding noise directly to real data produces poisoned data whose attack quality is very difficult to control. Intuitively, better attack effectiveness can be achieved by making a noise level higher, but this can make the noise more noticeable and thus leading to worse attack stealthiness. This is because the manually added noise (e.g. Gaussian, Salt and Pepper (SAP)) has nothing related to the original data statistically. In contrast, the noise generation of VagueGAN is guided by the statistics of original data, so that the GAN-generated noise can more smoothly fit the original data. Our experiments will show that only VagueGAN can flexibly control the quality of vague data on demand to strike a balance between attack effectiveness and stealthiness.

B. VagueGAN Poisoning Attack

Following the workflow of VagueGAN in Figure 2, the attacker first gains control over a client c_j and deploys an untrained VagueGAN model. The compromised client then functions as a malicious participant in the FL process. Before federated training starts, the malicious client trains the VagueGAN model on its local dataset using the loss function defined in Eq. (1). The training process of VagueGAN is similar to those of traditional GANs, where the generator and discriminator undergo iterative optimization through an adversarial game. Next, the trained VagueGAN model generates poisoned dataset $\mathcal{D}_j^{\text{poison}}$, which subsequently replaces the original dataset \mathcal{D}_j . Notably, the purpose of generating a poisoned dataset of the same size as the original dataset is just to ensure a fair comparison among different attack methods. That is, for every original data sample (x, y) , there exists exactly one corresponding poisoned sample (x^p, y) in the poisoned dataset. Finally, client c_j uses $\mathcal{D}_j^{\text{poison}}$ to train and upload a poisoned local model $\theta_{t,j}^{\text{poison}}$ to the server. Unlike a traditional attack such as label flipping that only affects selected labels, our VagueGAN indirectly attacks a global model with all labels/classes involved. The steps for conducting a VagueGAN poisoning attack are summarized in Algorithm 1.

C. Theoretical Analysis

This subsection theoretically reveals the characteristics of poisoned data generated by VagueGAN. For the expectation

Algorithm 1 VagueGAN poisoning attack algorithm

Input: Client c_j 's local training dataset $\mathcal{D}_j^{\text{train}}$
Output: Poisoned local training dataset $\mathcal{D}_j^{\text{poison}}$; local model parameters $\theta_{t,j}^{\text{poison}}$

- 1: **Initialization:** Number of training epochs E for VagueGAN; generator suppression factor κ ; number of training rounds T for FL
- 2: Deploy the VagueGAN model at a controlled client c_j and receive an FL training task from the server.
- 3: *//Poisoned Data Generation*
- 4: **for** $e = 1, 2, \dots, E$ **do**
- 5: Set training batch = $\mathcal{D}_j^{\text{train}}$
- 6: Train the VagueGAN model on $\mathcal{D}_j^{\text{train}}$ according to (1)
- 7: **end for**
- 8: Get outputted $\mathcal{D}_j^{\text{poison}}$
- 9: *//FL Training Task*
- 10: **for** $t = 1, 2, \dots, T$ **do**
- 11: Receive the global model $\tilde{\theta}_t$ from the server
- 12: Train the local model $\theta_{t,j}$ on $\tilde{\theta}_t$ and $\mathcal{D}_j^{\text{poison}}$
- 13: Get outputted $\theta_{t+1,j}^{\text{poison}}$ and upload it to the server
- 14: **end for**

form of the loss function in Eq. (1), we rewrite it in integral notation as follows:

$$\min_G \max_D V(G, D) = \int_{\mathbf{x}} p_d(\mathbf{x}) \log(1 + \kappa)D(\mathbf{x})d\mathbf{x} + \int_{\mathbf{z}} p_z(\mathbf{z}) \log(1 - (1 + \kappa)D(G(\mathbf{z})))d\mathbf{z}. \quad (2)$$

The data distribution learned by the generator G is represented as $p_g(\mathbf{x})$. According to the Law of the Unconscious Statistician (LOTUS) theorem, by replacing z using its mapping to \mathbf{x} and then transforming it into an integral form, we can obtain an alternative expression for Eq. (4):

$$\min_G \max_D V(G, D) = \int_{\mathbf{x}} [p_d(\mathbf{x}) \log(1 + \kappa)D(\mathbf{x}) + p_g(\mathbf{x}) \log(1 - (1 + \kappa)D(\mathbf{x}))]d\mathbf{x}. \quad (3)$$

For a fixed generator G , our objective is to solve for $\max_D V(G, D)$, which entails finding the optimal discriminator D^* that maximizes the right-hand side of the equation.

$$\max_D V(G, D) = \int_{\mathbf{x}} [p_d(\mathbf{x}) \log(1 + \kappa)D(\mathbf{x}) + p_g(\mathbf{x}) \log(1 - (1 + \kappa)D(\mathbf{x}))]d\mathbf{x}. \quad (4)$$

In Eq. (4), $p_d(\mathbf{x})$ refers to the probability of sampling a sample \mathbf{x} from the distribution p_d , $p_g(\mathbf{x})$ refers to the probability of sampling a sample from the generator G , and $D(\mathbf{x})$ represents a mapping of $x \in \mathbb{R}$. The maximization of the integral in Eq. (4) can be reformulated as finding the maximum value of the integrand, through determining the optimal discriminator D . Consequently, during this process, the probabilities associated with the real data distribution $p_d(\mathbf{x})$ and the generated data distribution $p_g(\mathbf{x})$ can be treated as constants. Taking the

partial derivatives of both sides of the equation with respect to D , we obtain:

$$\begin{aligned} \frac{\partial}{\partial D} (\max_D V(G, D)) &= \int_{\mathbf{x}} \frac{\partial}{\partial D} [p_d(\mathbf{x}) \log((1 + \kappa)D(\mathbf{x})) \\ &\quad + p_g(\mathbf{x}) \log(1 - (1 + \kappa)D(\mathbf{x}))]d\mathbf{x} \quad (5) \\ &= \int_{\mathbf{x}} \left[p_d(\mathbf{x}) \frac{1}{D(\mathbf{x})} + p_g(\mathbf{x}) \frac{-(1 + \kappa)}{1 - (1 + \kappa)D(\mathbf{x})} \right] d\mathbf{x}. \end{aligned}$$

By taking further derivatives of Eq. (5), it can be determined that Eq. (4) is a convex function. Therefore, Eq. (4) attains a unique maximum value at the point where its first derivative is equal to zero. At this point:

$$D^*(\mathbf{x}) = \frac{p_d(\mathbf{x})}{(1 + \kappa)(p_d(\mathbf{x}) + p_g(\mathbf{x}))}. \quad (6)$$

When $D^*(\mathbf{x}) = 0.5$, the specially designed discriminator in VagueGAN is unable to distinguish between real samples and fake samples generated by the generator. At this point, the generator of VagueGAN reaches its generation bottleneck. Consequently, one can conclude that:

$$p_g(\mathbf{x}) = \frac{(1 - \kappa)}{(1 + \kappa)}p_d(\mathbf{x}). \quad (7)$$

Eq. (7) reveals that VagueGAN has a distinct generation objective compared to traditional GANs. When VagueGAN achieves optimal performance, the distribution of the generated poisoned data is related to the original data distribution, but not identical. This distinction arises from the unique suppression factor κ in VagueGAN. By adjusting the suppression factor κ , VagueGAN can control the level of conformity between the generated poisoned data and the real data. Within the feasible range of κ ($\kappa \in (0, 1)$), a higher value of κ leads to a reduced correlation between the poisoned data and the real data, while a lower value of κ yields a higher correlation. When κ equals 0, VagueGAN is equivalent to a regular GAN.

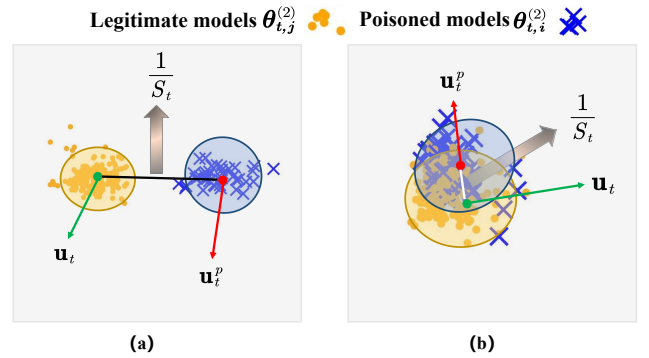


Fig. 3: Different levels of attack stealthiness: (a) Lower attack stealthiness for larger inter-cluster distance; (b) Higher attack stealthiness for smaller inter-cluster distance.

D. Attack Effectiveness-Stealthiness Trade-off

There is usually a trade-off between attack effectiveness and stealthiness. Noisier data generated by VagueGAN can be more effective in degrading FL performance, but may bring greater statistical changes and thus may be easier to detect. Therefore, the attacker needs to make appropriate settings for VagueGAN to fine-tune the quality of vague data and

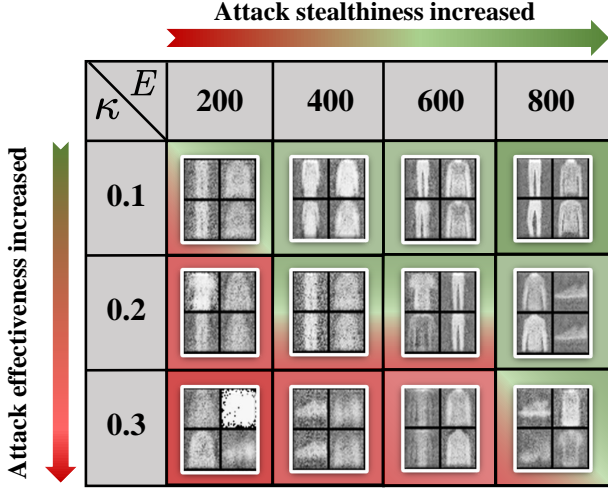


Fig. 4: Trade-off between attack effectiveness and stealthiness: Higher effectiveness but lower stealthiness for the lower left region, while lower effectiveness but higher stealthiness for the upper right region.

achieve a balanced trade-off between attack effectiveness and stealthiness. Here we give some guidelines for taking full advantage of VagueGAN for the balanced trade-off.

The effectiveness A_t of an attack in round t of FL can be characterized by the drop in the accuracy of the global model from a_t to a_t^p due to the presence of the attack:

$$A_t = a_t - a_t^p. \quad (8)$$

For a multi-class classification task, we employ the one-vs-rest strategy to compute the overall accuracy metric a_t :

$$a = \frac{\sum_{i=1}^l (TP_{t,i} + TN_{t,i})}{\sum_{i=1}^l (TP_{t,i} + TN_{t,i} + FP_{t,i} + FN_{t,i})} \quad (9)$$

where l denotes the total number of classes. For each class i , if we treat it as the positive and all the other classes as the negative, we can easily compute the numbers of true positives (TP_i), true negatives (TN_i), false positives (FP_i), and false negatives (FN_i), respectively, and finally the overall accuracy.

The stealthiness S_t of an attack in round t of FL can be characterized by the statistical distance between the clusters of legitimate and poisoned models. Since every local model $\theta_{t,i}$ is very high-dimensional, we first use PCA to downscale $\theta_{t,i}$ to 2-dimensional $\theta_{t,i}^{(2)}$.

$$\theta_{t,i}^{(2)} = \text{PCA}(\theta_{t,i}). \quad (10)$$

Then, we separate all legitimate local models and poisoned local models into two clusters and find the centroids \mathbf{u}_t and \mathbf{u}_t^p of these two clusters, respectively.

$$\mathbf{u}_t = \frac{\sum_{i=1}^{N-M} \theta_{t,i}^{(2)}}{N-M} \quad (11)$$

$$\mathbf{u}_t^p = \frac{\sum_{j=1}^M \theta_{t,j}^{(2)}}{M} \quad (12)$$

where N is the number of all clients and M is the number of malicious clients, so $N - M$ is the number of benign clients.

We use the reciprocal of the Euclidean distance \mathbf{E} between \mathbf{u}_t and \mathbf{u}_t^p to measure S_t :

$$S_t = \frac{1}{\mathbf{E}(\mathbf{u}_t, \mathbf{u}_t^p)} = \frac{1}{\|\mathbf{u}_t - \mathbf{u}_t^p\|}. \quad (13)$$

Specifically, this study employs the centroid linkage definition under the Euclidean distance metric. Note that it also supports other inter-cluster distance definitions such as single linkage, complete linkage, or average linkage, or other distance metrics such as cosine similarity. Figure 3 illustrates two cases with different levels of attack stealthiness. The performance of S_t is lower (or higher) as in Figure 3(a) (or 3(b)) when the statistical distance between legitimate and poisoned models is larger (or smaller).

To study the trade-off between attack effectiveness A_t and stealthiness S_t , we have analyzed the experimental outputs of VagueGAN, as in Figure 4. Clearly, the trade-off is closely related to the quality of poisoned data generated by VagueGAN. The more VagueGAN learns the characteristics of legitimate data, the higher stealthiness but lower effectiveness the resulting attack can achieve, and vice versa. In Figure 4, there are three general attack outcomes given by VagueGAN: low effectiveness/high stealthiness (upper right region), high effectiveness/low stealthiness (lower left region), and balanced effectiveness/stealthiness (central region). Due to the mutually exclusive nature of effectiveness and stealthiness, achieving both high effectiveness and high stealthiness by an attack is relatively unfeasible. Hence, the balanced outcome can be a rational goal for the attacker.

In follow-up experiments, it has been found that there are two important factors affecting the quality of poisoned data: VagueGAN training epochs E and generator suppression factor κ . A balanced trade-off between attack effectiveness A_t and stealthiness S_t can be achieved by setting the values of E and κ appropriately. E is set to make VagueGAN stay in a semi-fitting state, and κ is adjusted to limit the generation ability of the generator of VagueGAN. For example, poisoned data of balanced quality around the middle area in Figure 4 can be generated by experimentally setting $E \in [400, 600]$ and $\kappa = 0.2$. This configuration aims to achieve the ideal state of median effectiveness/median stealthiness. More details can be found in subsection VI-C.

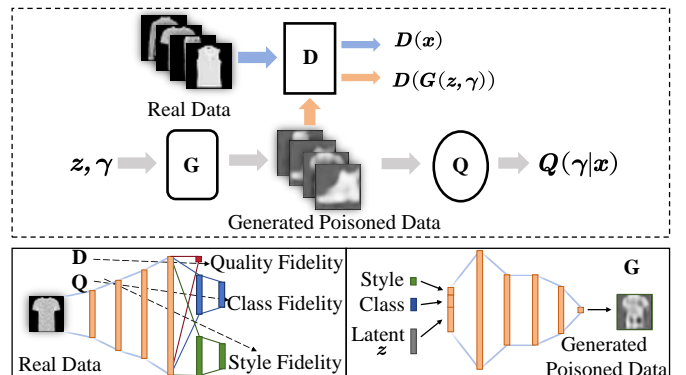


Fig. 5: Architecture of unsupervised VagueGAN: An extra classifier network Q measures the validity of auxiliary vector.

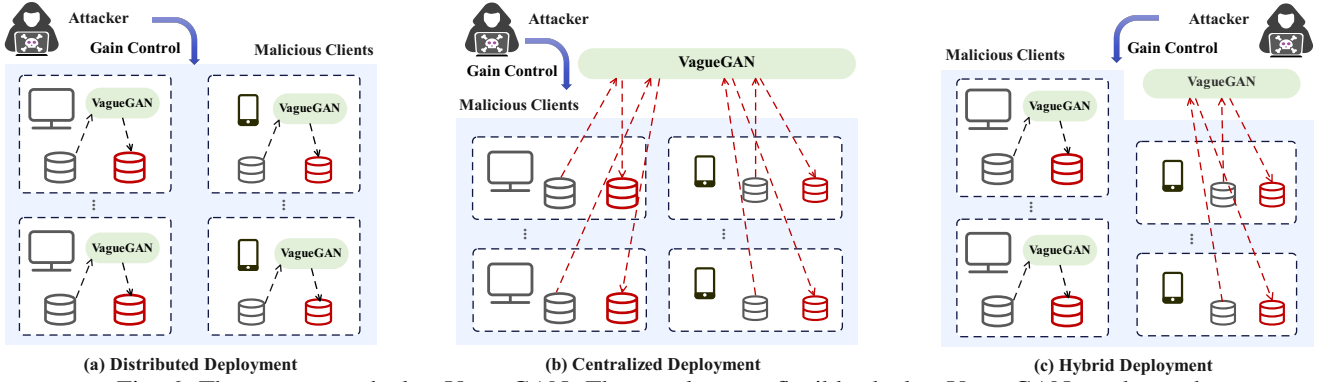


Fig. 6: Three ways to deploy VagueGAN: The attacker can flexibly deploy VagueGAN on demand.

E. Unsupervised Variant of VagueGAN

Sometimes the attacker may not have full access to the label information of a local dataset, making the generation of poisoned data even more challenging. Inspired by InfoGAN, we further propose an unsupervised variant of VagueGAN for broader applicability. As shown in Figure 5, unsupervised VagueGAN could not only learn to generate realistic samples but also learn auxiliary features (class fidelity and style fidelity). Similar to supervised generation, unsupervised VagueGAN also replaces the original distribution of data with a conditional distribution. The main difference lies in that unsupervised VagueGAN does not require feeding label and attribute information into the discriminator network. Instead, it utilizes another classifier Q to learn auxiliary features.

As shown in Figure 5, both the discriminator and generator networks of unsupervised VagueGAN consist of 4 hidden layers. Unsupervised VagueGAN uses an additional classifier network Q to measure the validity of the auxiliary vector. This additional classifier shares most of its weights (the first 4 hidden layers) with the discriminator.

The objective of unsupervised VagueGAN is defined as follows, with an addition $-\lambda L(G, Q)$, to Eq. (1):

$$\begin{aligned} \min_{G, Q} \max_D V(G, D, Q) &= \mathbb{E}_{x \sim p_d(x)} [\log(1 + \kappa) D(x)] + \\ &\mathbb{E}_{z \sim p_z(z), \gamma \sim p(\gamma)} [\log(1 - (1 + \kappa) D(G(z, \gamma)))] \\ &- \lambda L(G, Q) \end{aligned} \quad (14)$$

where λ is hyperparameter, $x \sim G(z, \gamma)$ is the generated poisoned data, and γ represents auxiliary information, which includes class fidelity and style fidelity generated from classifier Q . $p(\gamma)$ describes the actual distribution of γ , which is rather hard to obtain. Therefore, VagueGAN uses the posterior distribution, $Q(\gamma|x)$, to estimate $p(\gamma)$, and this process is done with a neural network classifier. $L(G, Q)$ is an approximation of mutual information (lower bound of mutual information), $I(\gamma; G(z, \gamma))$, between the auxiliary vector and generated poisoned sample:

$$\begin{aligned} L(G, Q) &= \mathbb{E}_{\gamma \sim p(\gamma), x \sim G(z, \gamma)} [\log Q(\gamma|x)] + H(\gamma) \\ &= \mathbb{E}_{x \sim p_G(x|z, \gamma)} E_{\gamma \sim p(\gamma|x)} \log Q(\gamma|x) + H(\gamma) \\ &\leq I(\gamma; G(z, \gamma)). \end{aligned} \quad (15)$$

Mutual information, $I(\gamma; G(z, \gamma))$, describes how much VagueGAN knows about random variable γ based on knowledge of $G(z, \gamma)$, i.e. $I(\gamma; G(z, \gamma)) = H(\gamma) - H(\gamma|G(z, \gamma))$,

in which $H(\gamma)$ is conditional entropy. It can also be described by the Kullback-Leibler divergence, the information loss when using marginal distributions to approximate the joint distribution of γ and $G(z, \gamma)$.

Thanks to the unique loss function, the effectiveness and stealthiness of supervised and unsupervised VagueGAN attacks are comparable. Detailed evaluation results can be found in subsection VI-D.

F. Deployment Advantages

VagueGAN can be readily deployable in practice. First, VagueGAN is relatively easy to train. VagueGAN introduces a unique loss function that prevents from generating high-quality data unnecessary for attack purpose. In addition, VagueGAN does not have to wait for the convergence to a Nash equilibrium to obtain relatively low-quality but damaging poisoned data, leading to substantially reduced training efforts and costs compared to regular GANs. The adoption of full dataset training also demands fewer epochs to generate expected poisoned data. The limitations inherent to a regular GAN, such as non-convergence and unstable training, do not hinder the use of VagueGAN. In comparison, the original GAN is unable to generate data that meets the requirements for poisoning attacks. Even its intermediate outputs during the generation process can only achieve a degree of "vagueness" without carrying "noise". Additionally, even with simpler models, achieving its generation goal is associated with high training costs. Second, VagueGAN only incurs one-time cost. It requires to build up a loss function from available datasets only once, enabling the generation of an arbitrary amount of poisoned data thereafter. Third, VagueGAN can be flexibly deployed depending on the attacker's resource availability. In general, there are three ways to put VagueGAN into use, including distributed deployment, centralized deployment, and hybrid deployment, so it is not hard for the attacker to find a way to deploy VagueGAN.

Distributed Deployment: As shown in Figure 6(a), if the attacker has gained the control of one or more clients with rich on-device resources, a VagueGAN model can be individually trained on each of the malicious clients, giving diversified poisoned datasets. When we use the term "VagueGAN" in this paper, we will mean VagueGAN implementing a distributed deployment, unless we state otherwise.

Centralized Deployment: As shown in Figure 6(b), if the attacker has access to a resource-rich platform reachable from

the clients, one or more VagueGAN models can be centrally trained after collecting local data from the malicious clients. Then either unified or diversified poisoned datasets can be distributed to the malicious clients.

Hybrid Deployment: As shown in Figure 6(c), if some of the malicious clients have rich on-device resources but others do not, a mixture of locally trained and centrally trained VagueGAN models can be applied.

V. MODEL CONSISTENCY-BASED DEFENSE

Thanks to its inherent generative capability, our VagueGAN can generate seemingly legitimate poisoned data and thus can bypass existing defense methods. In this section, we analyze the characteristics of GAN outputs and suggest a model consistency-based countermeasure to stealthier GAN-based data poisoning attacks. Our defense method is effective when the same VagueGAN model is consistently applied by the attacker, though the idea of VagueGAN still has great potential to deliver undetectable attacks if implemented in varying settings. Moreover, our defense method also works well against mainstream data poisoning attacks.

A. Local Model Analysis

To find a clue for the identification of malicious clients given that the server does not have access to any local data, we analyze the statistical patterns of local models successively uploaded by a certain client within a certain time span.

Due to the high-dimensional characteristics of local models, it would be difficult to review them directly and the review process would impose a huge computational load on the server. To better analyze the local models, we use PCA to reduce the high-dimensional models to 2-dimensional ones to extract the most useful information. Typical distributions of legitimate and poisoned models after PCA are compared in Figure 7, and the corresponding experimental details can be found in section VI.

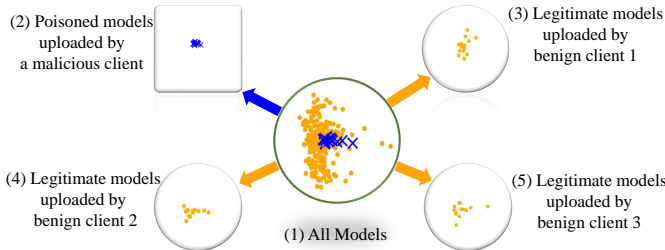


Fig. 7: Legitimate and poisoned models after PCA: Higher model consistency can be observed for poisoned models compared with legitimate ones.

It can be seen that the distribution of poisoned models given by the VagueGAN model is close to those of legitimate models except for their distribution density or consistency levels. The poisoned models uploaded by the same malicious client are more densely distributed within a smaller region. This is mainly caused by the consistency of GAN outputs, as GAN-generated data usually have a certain degree of data feature similarity. Malicious clients keep using similar GAN-poisoned data train poisoned models, and the consistency of GAN outputs further leads to the consistency of the corresponding poisoned models. Inspired by this observation, we propose to

identify malicious clients by examining the consistency level of local models successively uploaded by every client.

B. MCD Design

In order to address the stealthier data poisoning attacks, we propose a new defense method named Model Consistency-Based Defense (MCD), which is performed by the server in four steps. The specific process is as follows:

a) Step 1 (Model Processing): MCD maintains a trusted set of clients, denoted as C^{tr} . Here, C^{tr} refers to a collection of clients that are temporarily considered to be benign in the system. During the initialization phase, C^{tr} is set to \mathcal{C} . MCD runs periodically for every defense period of T' FL rounds for local model analysis. In each defense period, MCD stores a set $\mathcal{Q}_{f,i}$ of low-dimensional local models uploaded by every trusted client $c_i \in C^{\text{tr}}$ to the server in T' rounds, $f = 0, 1, 2, 3, \dots$ stands for the f th defense period, thus $f = \lfloor \frac{t}{T'} \rfloor$. Here we take 2-dimensional models after dimensionality reduction by PCA as an example, but MCD is not limited to it. In our FL system, the server randomly selects K out of N clients per round for model aggregation, so $\theta_{t,i}^{(2)} \in \mathcal{Q}_{f,i}$ is set to $NULL$ if client c_i is not selected in round t . MCD identifies malicious clients and removes them from C^{tr} in each defense.

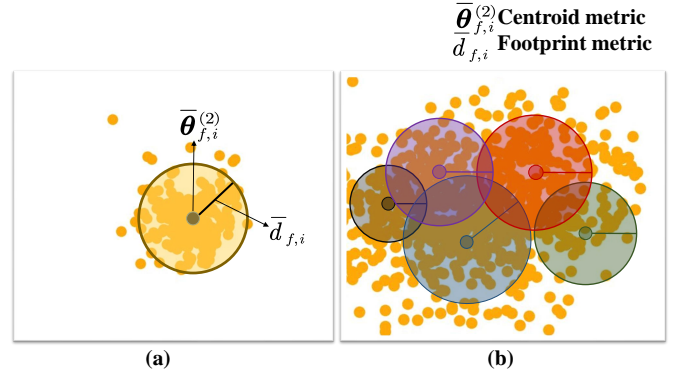


Fig. 8: Two metrics for model consistency evaluation: A centroid metric $\bar{\theta}_{f,i}^{(2)}$ and a footprint metric $\bar{d}_{f,i}$.

Afterward, MCD utilizes two crucial metrics calculated from $\mathcal{Q}_{f,i}$ of each trusted client c_i to evaluate a model consistency level. First, for each trusted client c_i , MCD calculates a centroid metric :

$$\bar{\theta}_{f,i}^{(2)} = \frac{\sum_{\theta_{t,i}^{(2)} \in \mathcal{Q}_{f,i}} \theta_{t,i}^{(2)}}{|\mathcal{Q}_{f,i}|} \quad (16)$$

where $\bar{\theta}_{f,i}^{(2)}$ represents the center of all models uploaded by a single client c_i (shown in Figure 8(a)). Anomalies with the centroid metric can be used to detect most of the existing data poisoning attacks, such as label flipping attacks, PoisonGAN, noise superimposition attack, etc, as validated in subsection VI-D. Second, MCD calculates a footprint metric

$$\bar{d}_{f,i} = \frac{\sum_{\theta_{t,i}^{(2)} \in \mathcal{Q}_{f,i}} \|\theta_{t,i}^{(2)} - \bar{\theta}_{f,i}^{(2)}\|}{|\mathcal{Q}_{f,i}|} \quad (17)$$

where $\bar{d}_{f,i}$ is the mean of the Euclidean distances, i.e., variances, of all models from the centroid $\bar{\theta}_{f,i}^{(2)}$. A circular region

Algorithm 2 Client abnormality evaluation algorithm

Input: Trusted client set \mathcal{C}^{tr} ; baseline client set $\mathcal{C}^{\text{base}}$
Output: All trusted clients' abnormality set \mathcal{H}_f
Initialization: Weights of two anomalous terms λ_1, λ_2

```

1: //Calculate Baseline Values
2: for  $c_i \in \mathcal{C}^{\text{base}}$  do
3:   Calculate the base value  $\theta_f^{\text{base}}$  according to (20)
4:   Calculate the base value  $d_f^{\text{base}}$  according to (21)
5: end for
6: //Calculate Abnormal Degree
7: for  $c_i \in \mathcal{C}^{\text{tr}}$  do
8:   Calculate the client abnormality  $h_{f,i}$  with  $\lambda_1, \lambda_2$  according to (21)
9:   Get outputted trusted client  $c_i$ 's abnormality  $h_{f,i}$ 
10: end for
11: Output all trusted clients' abnormality set  $\mathcal{H}_f$ 

```

defined by $\bar{\theta}_{f,i}^{(2)}$ as the center and $\bar{d}_{f,i}$ as the radius represents a simplified footprint of the client c_i 's model distribution (shown in Figure 8(a)). Anomalies with the footprint metric can be used to detect GAN-based data poisoning attacks when the same GAN model like VagueGAN is applied consistently. Each pair of centroid and footprint metrics is extracted from a set of high-dimensional local models, and MCD can cost-effectively work with such extracted metrics instead of the original models. This greatly saves the storage space of the server, and also keeps the computational effort of MCD low to identify malicious clients.

Thus far, MCD pre-processes each trusted client c_i 's local models into a pair of two key metrics ($\bar{\theta}_{f,i}^{(2)}, \bar{d}_{f,i}$). Figure 8(b) presents an example of five clients' metric pairs.

b) Step 2 (Baseline Value Calculation): MCD calculates baseline values $\theta_f^{\text{base}}, d_f^{\text{base}}$ of above two metrics for anomaly detection. The calculation of baseline values is a crucial step in MCD as it directly influences the effectiveness of its judgment.

Thus, MCD establishes a baseline client set $\mathcal{C}^{\text{base}}$ for baseline values calculation, and the processes of selecting the baseline clients are as follows. Firstly, MCD maintains a first baseline client (for instance, the server acts as a such client to train a local model). This client is considered 100% secure and immune to attacks, and its model metrics are denoted as $(\hat{\theta}_f^{(2)}, \hat{d}_f)$. The first baseline client can expand to multiple ones if possible. Secondly, MCD defines $\mathcal{C}^{\text{base}}$ as the set of baseline clients whose model metrics are within a neighborhood of those of the first baseline client. Two constants Ω_1, Ω_2 are used to define the size of the neighborhood:

$$\frac{\|\bar{\theta}_{f,i}^{(2)} - \hat{\theta}_f^{(2)}\|}{\hat{d}_f} < \Omega_1 \quad (18)$$

which represents the requirement for the centroid metrics, and

$$\frac{|\bar{d}_{f,i} - \hat{d}_f|}{\hat{d}_f} < \Omega_2 \quad (19)$$

which represents the requirement for the footprint metrics.

After filtering out the baseline client set $\mathcal{C}^{\text{base}}$ based on the above constraints, MCD utilizes the model metrics of

Algorithm 3 MCD defense algorithm

Input: All clients' model set $\mathcal{Q}_f = \{\mathcal{Q}_{f,1}, \mathcal{Q}_{f,2}, \dots, \mathcal{Q}_{f,i}, \dots, \mathcal{Q}_{f,N}\}$
Output: Trusted client set \mathcal{C}^{tr}
Initialization: Defense period of MCD T' ; Trusted client set $\mathcal{C}^{\text{tr}} = \mathcal{C}$

```

1: for  $t = 1, 2, \dots, T$  do
2:   if  $t \% T' \neq 0$  then
3:      $f = \lfloor \frac{t}{T'} \rfloor$ 
4:     for  $\mathcal{Q}_{f,i} \in \mathcal{Q}_f$  do
5:       Calculate model metrics  $\bar{\theta}_{f,i}^{(2)}, \bar{d}_{f,i}$  according to (15),(16)
6:       Use  $(\bar{\theta}_{f,i}^{(2)}, \bar{d}_{f,i})$  instead of  $\mathcal{Q}_{f,i}$ 
7:     end for
8:     Select baseline client set  $\mathcal{C}^{\text{base}}$  according to (18)(19)
9:     Run Algorithm 2: Client abnormality evaluation
10:    Get outputted  $\mathcal{H}_f$ 
11:    Calculate  $h_f^{\text{thr}}$  according to (23)
12:    for  $c_i \in \mathcal{C}^{\text{tr}}$  do
13:      if  $h_{f,i} > h_f^{\text{thr}}$  then
14:        remove  $c_i$  from  $\mathcal{C}^{\text{tr}}$ 
15:        remove  $\mathcal{Q}_{f,i}$  from  $\mathcal{Q}_f$ 
16:      end if
17:    end for
18:  end if
19:  Update  $\mathcal{C}^{\text{tr}}, \mathcal{Q}_f$ 
20: end for

```

the baseline clients to calculate the baseline values. The calculation of θ_f^{base} is as follows:

$$\theta_f^{\text{base}} = \frac{\sum_{\bar{\theta}_{f,i}^{(2)} \in \mathcal{C}^{\text{base}}} \bar{\theta}_{f,i}^{(2)}}{|\mathcal{C}^{\text{base}}|}. \quad (20)$$

Similarly, the calculation process of d_f^{base} is as follows:

$$d_f^{\text{base}} = \frac{\sum_{\bar{d}_{f,i} \in \mathcal{C}^{\text{base}}} \bar{d}_{f,i}}{|\mathcal{C}^{\text{base}}|}. \quad (21)$$

So far, MCD has obtained the centroid baseline value θ_f^{base} and the footprint baseline value d_f^{base} .

c) Step 3 (Client Abnormality Calculation): MCD uses the baseline values to calculate every trusted client abnormality separately. That is to calculate the degree of deviation of each client c_i 's metric pair $(\bar{\theta}_{f,i}^{(2)}, \bar{d}_{f,i})$ from the baseline values. MCD quantifies it as $h_{f,i}$, and the calculation of $h_{f,i}$ is:

$$h_{f,i} = \lambda_1 \left(\frac{\|\bar{\theta}_{f,i}^{(2)} - \theta_f^{\text{base}}\|}{d_f^{\text{base}}} \right) + \lambda_2 (|d_f^{\text{base}} - \bar{d}_{f,i}|). \quad (22)$$

The client abnormality set of all trusted clients is denoted as \mathcal{H}_f . The first part of $h_{f,i}$ can be used to detect anomalies with the centroid metric, while the second part can be used to detect anomalies with the footprint metric. λ_1, λ_2 are weights and can be set as needed. The first half and the second half of Eq. (21) are not of the same order of magnitude. λ_1 and λ_2 are used to normalize the two parts. The steps for client abnormality evaluation are summarized in Algorithm 2.

d) Step 4 (Malicious Client Identification): After obtaining all trusted client abnormality values, MCD finds a median value say h_f^{med} . MCD then calculates an abnormality threshold h_f^{thr} for malicious client detection:

$$h_f^{\text{thr}} = \delta h_f^{\text{med}} \quad (23)$$

where parameter $\delta \in (1, 3)$ controls the threshold. MCD then marks every client with a client abnormality value larger than the threshold as a malicious client. If MCD detects a malicious client, it will be removed from the trusted client set \mathcal{C}^{tr} . The complete procedure of MCD, executed by the server, is outlined in Algorithm 3.

Overall, MCD is well-equipped to work against GAN-based data poisoning attacks as well as other mainstream ones. MCD run by the server takes advantage of a sufficient number of collected local models to conduct feature extraction so as to derive the two key metrics for model consistency evaluation. The centroid metric is useful for detecting most of the existing data poisoning attacks, such as label flipping, PoisonGAN, and noise superimposition, while the footprint metric is powerful for detecting GAN-based data poisoning attacks. As summarized in Tables II and III, MCD is more widely effective than existing defense methods.

In addition, MCD can be implemented in a cost-effective manner. MCD operates without model collection overhead, since it directly reuses the local models already collected by the server for federated aggregation. Furthermore, on the premise of ensuring that the accuracy of judgment is not affected, some measures have been taken to ensure minimum impact on the server load: 1) MCD works with extracted metrics instead of original high-dimensional models, which avoids high space load on the server. 2) MCD uses a lightweight anomaly detection algorithm, which does not require complex computations. 3) MCD defends every period of tens of training rounds rather than every round, which avoids high computational load on the server.

VI. PERFORMANCE EVALUATION

In this section, we evaluate our presented VagueGAN and MCD through extensive experiments on multiple open real-world datasets.

A. Experimental Settings

a) Datasets and Learning Task: We take image data as an example to evaluate the poisoning capability of our VagueGAN, but the idea of “vague data” is not limited to this specific data type. We conduct our experiments on five typical real-world datasets: MNIST, Fashion-MNIST, CIFAR-10, CIFAR-100, and Mini-ImageNet. These datasets are commonly used in existing works. The learning task of our FL system is to train a deep learning model for image classification. In the experiments using MNIST and Fashion-MNIST, a CNN with two convolutional layers (16 and 32 channels, 5×5 kernels, padding 2), each followed by batch normalization, ReLU, and 2×2 max pooling, is used. A fully connected layer maps the $7 \times 7 \times 32$ features to 10 classes. In the experiments using CIFAR-10, a CNN with six convolutional layers (using 3×3

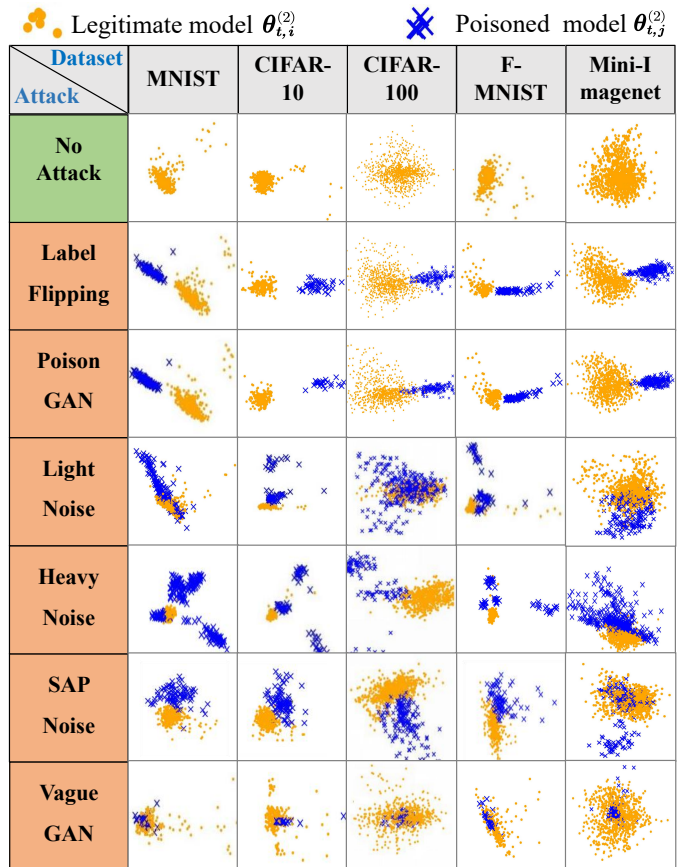


Fig. 9: Two-dimensional local model visualization: VagueGAN shows higher stealthiness than the others due to a shorter distance between legitimate and poisoned models.

kernels and padding 1), grouped into three blocks with 32, 64, and 128 channels respectively, each block followed by batch normalization, ReLU activation, and 2×2 max pooling, is used. Two fully connected layers map the $4 \times 4 \times 128$ features to 10 output classes. The model used for CIFAR-100 shares the same depth but has twice the width (i.e., number of channels) compared to that used for CIFAR-10, in order to better handle the higher number of classes. In the experiments using Mini-ImageNet, we employ a CNN with three convolutional blocks having 64, 128, and 256 channels, respectively. Uniquely, this architecture incorporates an adaptive average pooling layer to standardize feature dimensions to 4×4 , followed by a dropout layer and two fully connected layers for 100-class classification.

b) Federated Learning Setup: We utilize the PyTorch package to implement FL in Python. The FL system consists of $N = 60$ clients by default and a central server, which randomly chooses $K = 10$ clients per round for model aggregation. Each training process of FL lasts $T = 200$ rounds. Each training dataset is split into N partitions as the clients’ local datasets, which can be either IID or non-IID. The non-IID case is set according to [35].

c) Attack Methods: The four data poisoning attack methods in comparison are set up as follows.

(1) *Label flipping attack* [3]: This method flips specific labels of training data to achieve targeted data poisoning in FL. Specifically, the attacker poisons a local dataset as follows: For

TABLE I: Test accuracy under various data poisoning attacks (%) on different datasets: The 0% column is for the case without any attack, while the other columns are for the cases with different proportions of malicious clients in the FL system.

Client data distribution	IID					non-IID				
	Malicious Clients Percentage α									
Poisoning Attack	0%	5%	10%	20%	30%	0%	5%	10%	20%	30%
MNIST										
Label Flipping	98.73	98.65	98.48	98.32	98.11	98.39	98.32	98.08	97.92	97.59
Label Flipping+PoisonGAN	98.73	98.64	98.43	98.21	98.04	98.39	98.3	97.91	97.88	97.44
Light Noise Superimposition	98.73	98.66	98.57	98.41	98.31	98.39	98.37	98.15	98.02	97.74
Heavy Noise Superimposition	98.73	98.63	98.49	98.37	98.11	98.39	98.36	98.03	97.89	97.61
SAP Noise Superimposition	98.73	98.70	98.62	98.56	98.43	98.39	98.37	98.19	98.04	97.82
Cosine Noise Superimposition	98.73	98.69	98.60	98.45	98.24	98.39	98.39	98.15	98.00	97.18
VagueGAN	98.73	98.61	98.35	97.84	97.46	98.39	98.13	97.94	97.77	97.37
Fashion-MNIST										
Label Flipping	87.97	87.73	87.20	86.01	85.48	87.25	86.73	86.18	85.31	84.36
Label Flipping+PoisonGAN	87.97	87.59	87.17	85.77	85.09	87.25	86.59	86.01	85.04	84.08
Light Noise Superimposition	87.97	87.81	87.58	86.92	86.57	87.25	87.08	86.82	86.29	85.72
Heavy Noise Superimposition	87.97	87.71	87.15	86.16	85.56	87.25	86.94	86.57	85.83	85.33
SAP Noise Superimposition	87.97	87.80	87.52	86.99	86.43	87.25	87.12	86.77	86.32	85.94
Cosine Noise Superimposition	87.97	87.78	87.48	86.79	86.50	87.25	87.08	86.65	86.40	85.71
VagueGAN	87.97	87.34	86.79	85.87	84.77	87.25	86.64	85.84	84.91	84.02
CIFAR-10										
Label Flipping	76.28	75.69	74.99	73.86	72.85	73.61	72.32	71.23	70.18	68.78
Label Flipping+PoisonGAN	76.28	75.62	74.84	73.77	72.66	73.61	72.16	71.06	70.04	68.66
Light Noise Superimposition	76.28	76.03	75.71	74.93	74.07	73.61	72.94	72.03	71.26	70.53
Heavy Noise Superimposition	76.28	75.88	75.13	74.24	73.11	73.61	72.82	71.88	70.73	69.94
SAP Noise Superimposition	76.28	76.12	75.73	74.71	73.96	73.61	72.99	71.97	71.22	70.38
Cosine Noise Superimposition	76.28	76.10	75.67	74.54	73.87	73.61	72.88	71.89	71.36	70.12
VagueGAN	76.28	74.94	74.02	73.16	71.93	73.61	71.96	70.64	69.55	67.79
CIFAR-100										
Label Flipping(x10)	55.71	53.03	52.52	49.25	46.68	53.43	52.07	49.26	46.78	41.39
Label Flipping+PoisonGAN	55.71	52.83	52.10	48.39	46.93	53.43	51.66	49.37	46.68	40.03
Light Noise Superimposition	55.71	54.03	53.67	51.08	49.95	53.43	52.92	50.97	48.50	45.95
Heavy Noise Superimposition	55.71	53.49	52.45	50.23	48.58	53.43	51.29	48.62	45.05	42.98
SAP Noise Superimposition	55.71	54.12	53.80	51.21	49.63	53.43	51.72	49.97	48.43	44.68
Cosine Noise Superimposition	55.71	54.37	53.53	51.17	49.15	53.43	51.67	49.61	48.48	43.56
VagueGAN	55.71	51.53	48.30	42.35	39.38	53.43	51.04	48.96	41.02	35.11
Mini-ImageNet										
Label Flipping(x10)	49.25	48.83	47.19	44.63	42.01	42.94	41.30	39.22	35.76	31.83
Label Flipping+PoisonGAN	49.25	48.30	46.92	43.75	41.40	42.94	40.89	37.08	33.81	30.42
Light Noise Superimposition	49.25	47.91	46.12	43.28	40.02	42.94	40.88	36.09	34.53	30.61
Heavy Noise Superimposition	49.25	46.98	44.16	39.81	36.17	42.94	38.29	34.41	30.71	25.67
SAP Noise Superimposition	49.25	46.59	45.59	41.39	38.22	42.94	40.00	36.67	31.99	27.30
Cosine Noise Superimposition	49.25	47.65	45.63	41.53	39.71	42.94	40.26	35.74	31.24	26.81
VagueGAN	49.25	46.12	41.16	35.22	29.35	42.94	37.33	32.24	27.06	19.76

all samples belonging to a source class, change their labels to another target class. In our experiment, every data sample with label “6” is given a poisoned label “0”.

(2) *Label flipping attack with PoisonGAN* [14]: A label flipping attack can work with PoisonGAN, an off-the-shelf GAN model used to enlarge the sizes of local datasets with legitimate pseudo samples by using a discriminator initialized by the global model. Note that PoisonGAN is just a data augmentation method used to enhance the label flipping attack, and it does not directly generate poisoned data. In our experiment, the malicious clients first enlarge their local datasets with pseudo data generated by PoisonGAN and then carry out a label flipping attack as above. The amount of pseudo data generated by PoisonGAN is 10% of each local dataset.

(3) *Noise superimposition attack* [36]: The attacker superimposes a certain type of noise on real data to generate poisoned data. Either light or heavy Gaussian noise is directly added to the original data, where light noise is with mean = 0 and variance = 0.1; heavy noise is with mean = 0 and variance = 0.3. In addition, SAP noise is added similarly, where 30% pixels of each image sample are noise-superimposed, and the proportion of “salt” versus “pepper” noise is 0.5. For cosine

noise [34], a perturbation pattern based on a cosine function is applied to the image data, with an amplitude of 2 and a frequency of 0.5.

(4) *VagueGAN*: For our VagueGAN, it generates the same amount of poisoned data as the real data, and replaces all the real data with the poisoned data. By default, let $\kappa = 0.2$, $E = 600$.

d) Defense Methods: In response to the above four data poisoning attacks, we compare the following defense methods.

(1) *PCA* [3]: This method constructs a local model list on the server, collecting all local models used for federated aggregation. After the local model list is constructed across $T' = 80$ rounds, it is standardized by zeroing the mean and being scaled to unit variance. The standardized list is fed into PCA for dimensionality reduction and visualization, and then clients with large outliers are labeled as malicious and subsequently ignored.

(2) *UMAP* [4]: This method follows the same logic as PCA, except for using UMAP for dimensionality reduction. As for its settings, neighborhood size for local structure approximation is 200, layout control parameter is 0.8, cosine distance is computed in the ambient space of input data.

TABLE II: Detection results of MCD under three attacks: Red indicates malicious clients; green indicates benign clients.

Scenario	Label flipping			PoisonGAN			Light noise superimposition		
	$\theta_f^{base}=(-5.31,-0.62), d_f^{base}=3.32$			$\theta_f^{base}=(-4.57,0.44), d_f^{base}=4.15$			$\theta_f^{base}=(-1.15, 0.25), d_f^{base}=2.72$		
i	$\bar{\theta}_{f,i}^{(2)}$	$\bar{d}_{f,i}$	$h_{f,i}$	$\bar{\theta}_{f,i}^{(2)}$	$\bar{d}_{f,i}$	$h_{f,i}$	$\bar{\theta}_{f,i}^{(2)}$	$\bar{d}_{f,i}$	$h_{f,i}$
0	(-6.22,4.26)	4.09	1.49	(19.61,-0.24)	3.68	6.77	(3.35,10.36)	3.89	6.41
1	(21.87,-0.58)	3.07	8.74	(-4.49,-0.33)	5.33	2.55	(-0.40,1.20)	2.53	0.82
2	(-1.86,-9.85)	3.79	2.97	(21.47,-0.52)	3.06	8.46	(2.66,2.45)	2.91	2
3	(-2.67,11.74)	3.13	4.18	(-4.73,-2.7)	4.46	1.38	(8.81,2.52)	5.08	8.48
4	(-3.58,3.63)	4.44	1.38	(-2.09,3.05)	4.62	1.81	(-1.10,0.05)	1.71	2.1
5	(-4.64,-3.19)	3.09	1.26	(-5.24,-1.12)	5.1	2.31	(-3.96,-2.02)	2.02	2.73
6	(-7.15,0.66)	3.43	0.67	(-3.13,1.56)	4.02	0.7	(13.32,-26.22)	4.04	13.71
7	(-6.87,-3.16)	2.85	1.84	(-3.22,6.41)	4.09	1.59	(-3.05,0.80)	3.88	3.05
8	(-4.59,-2.59)	3.2	0.87	(-6.38,4.06)	4.48	1.64	(1.40,-3.55)	2.37	2.38
9	(23.13,5.61)	3.14	9.13	(-5.93,0.64)	3.6	1.43	(-1.07,1.17)	3.9	2.7
10	(21.51,-4.57)	4.45	8.17	(22.25,-0.53)	3.31	8.15	(-4.34,3.92)	2.19	2.81
11	(-5.27,1.53)	3.92	0.65	(21.66,-0.57)	2.98	8.67	(-3.22,1.31)	1.68	2.94
12	(-3.44,-7.33)	3.03	2.67	(-3.95,2.86)	4.03	0.84	(-0.76,-1.64)	2.17	1.81
13	(-5.83,2.51)	3.3	0.99	(-5.07,1.43)	4.25	0.47	(-1.50,0.18)	1.37	2.83
14	(-4.82,-1.70)	2.84	1.34	(-6.55,4.28)	4.69	1.94	(-2.14,2.11)	2.7	0.82
15	(-7.19,-6.73)	2.78	3.26	(-5.73,-1.12)	4.32	0.81	(0.37,-1.00)	2.42	1.32
16	(-8.05,-6.00)	2.82	2.82	(-3.94,-2.67)	4.01	1.04	(2.60,1.76)	3.02	2.09
17	(-4.93,0.06)	2.97	0.93	(-3.32,-5.79)	4.22	1.71	(-1.63,-3.89)	2.3	2.35
18	(-7.89,0.25)	2.25	2.95	(-4.29,-5.14)	4.12	1.56	(-2.33,1.20)	1.12	1.12
19	(22.01,-0.43)	3.43	8.23	(-4.98,1.64)	4.65	1.31	(4.27,12.33)	3.75	6.89

TABLE III: Detection results of MCD under another three attacks.

Scenario	Heavy noise superimposition			SAP noise superimposition			VagueGAN		
	$\theta_f^{base}=(-0.51,-0.62), d_f^{base}=0.82$			$\theta_f^{base}=(-0.75,-3.70), d_f^{base}=1.50$			$\theta_f^{base}=(-0.05,0.02), d_f^{base}=5.55$		
i	$\bar{\theta}_{f,i}^{(2)}$	$\bar{d}_{f,i}$	$h_{f,i}$	$\bar{\theta}_{f,i}^{(2)}$	$\bar{d}_{f,i}$	$h_{f,i}$	$\bar{\theta}_{f,i}^{(2)}$	$\bar{d}_{f,i}$	$h_{f,i}$
0	(-0.81,-1.72)	0.73	1.48	(-2.32,-2.46)	1.9	2.8	(-2.52,0.93)	0.92	8.92
1	(0.01,-0.86)	0.75	0.77	(-13.38,14.01)	3.06	24.82	(-1.95,1.07)	1.01	8.64
2	(0.40,0.01)	0.76	1.41	(0.28,-6.14)	1.38	2.88	(-1.62,0.42)	6.13	0.32
3	(-0.30,0.09)	0.93	1.01	(1.23,-5.05)	1.41	2.57	(-2.77,4.45)	4.22	2.81
4	(32.10,-10.60)	6.22	46.98	(-1.61,-0.55)	2.42	5.1	(-0.19,-2.55)	4.31	2.12
5	(0.83,-1.00)	0.69	1.83	(-3.28,-2.26)	1.62	3.15	(0.01,-0.88)	3.29	3.49
6	(-0.87,-0.68)	0.8	0.46	(-1.55,-2.85)	1.56	1.28	(-0.40,-1.14)	3.68	3.11
7	(-22.62,-19.32)	6.18	40.68	(-0.41,-3.78)	1.2	0.9	(-2.45,-3.76)	4.3	2.51
8	(-7.12,28.24)	5.86	41.15	(-12.11,8.79)	2.6	19.09	(-2.01,0.32)	4.54	1.35
9	(-1.79,-0.92)	0.78	1.64	(-1.81,-3.06)	1.12	1.99	(3.34,-0.24)	6.45	0.66
10	(0.11,-0.87)	1.03	1.03	(35.53,9.16)	4.52	44.44	(-1.66,1.02)	1.35	7.9
11	(-0.88,-0.56)	0.85	0.48	(2.88,-6.84)	1.01	5.77	(-1.03,1.21)	6.59	0.3
12	(4.70,14.92)	4.92	24.09	(-1.02,-3.27)	1.24	1.02	(2.19,-0.11)	8.33	0.43
13	(-0.70,-1.48)	0.68	1.21	(-0.56,-2.42)	1.18	1.93	(2.69,-2.88)	6.42	0.77
14	(0.06,-0.57)	0.79	0.73	(-1.74,-4.62)	1.2	1.95	(-0.79,-0.03)	4.43	1.78
15	(0.31,-0.26)	0.83	1.11	(-1.98,-2.45)	2.52	3.79	(-0.56,0.74)	5.98	0.17
16	(-0.95,-0.48)	0.82	0.56	(-3.64,24.99)	3.87	33.57	(-1.58,4.02)	1.28	8.48
17	(-1.39,0.67)	0.9	1.92	(0.42,-6.47)	2.05	4.1	(3.56,2.36)	5.35	0.83
18	(-1.13,-0.28)	0.74	0.95	(0.13,-2.96)	1.05	2.04	(3.80,-3.04)	6.57	0.95
19	(-1.09,-1.00)	1.05	1.07	(-0.58,-4.17)	1.2	1	(2.91,-1.78)	8.26	0.67

(3) *CONTRA* [25]: This method builds upon the PCA-based defense by adding a cosine similarity analysis layer. After performing PCA dimensionality reduction, the cosine similarities between all pairs of clients' gradient vectors are computed. Clients with significantly deviated gradient directions are marked as malicious ones.

(4) *DnC* [22]: This method measures the directional divergence between gradient vectors in PCA space by computing the angles between client updates, identifying poisoned clients through statistically anomalous angular deviations.

(5) *LoMar* [6]: This method applies K-means clustering (with K=2) on PCA-reduced gradient vectors. After dimensionality reduction, it automatically identifies malicious clusters through two criteria: (a) cluster purity (flagging clusters with >80% poisoned clients) and (b) inter-cluster separation. The neighborhood size for local structure approximation follows the default settings of PCA.

(6) *FedDMC* [26]: This method implements a binary tree-

based clustering approach on PCA-reduced gradients. The algorithm first constructs a dendrogram using complete linkage hierarchical clustering, and then performs iterative binary splitting based on the maximum intra-cluster distance, while enforcing a minimum cluster size of 2. Potential poisoning clusters are identified when non-majority clusters contain $\geq 70\%$ known malicious clients. Distance computations use Euclidean norms in the reduced PCA space.

(7) *MCD*: For our MCD, parameters are set as follows. In MCD, the magnitude of the first part of $h_{f,i}$ in Eq. (21) is slightly larger than that of the second part. To balance the two anomaly evaluation components, we set $\lambda_1 = 1$ and $\lambda_2 = 2$. The number of FL rounds for a defense period is $T' = 80$. The constraints on the neighborhood for \mathcal{C}^{base} are $\Omega_1=4, \Omega_2=2$.

B. Attack Performance Comparison

In this subsection, we evaluate and compare the four attack methods in the same scenario, all of which are implemented

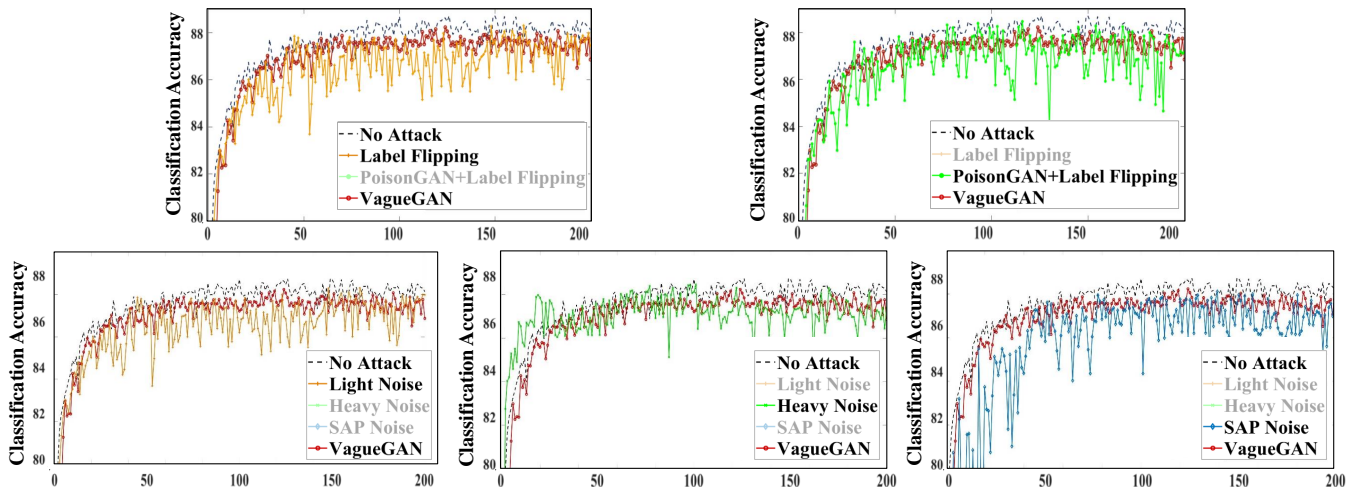


Fig. 10: Accuracy fluctuations of attack methods: VagueGAN shows less fluctuations in the global model’s test accuracy than the others, making it harder to detect.

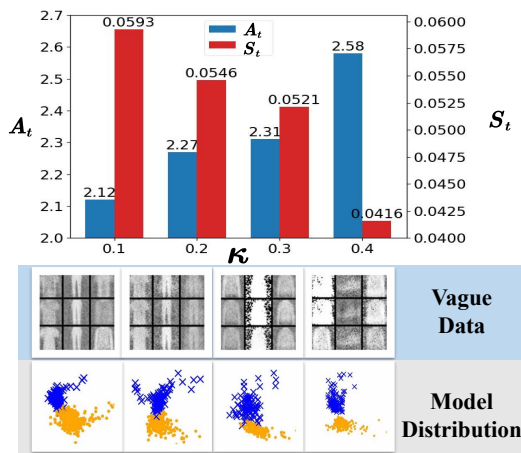


Fig. 11: Impact of suppression factor κ : A larger κ gives higher attack effectiveness but lower attack stealthiness.

to poison the same local datasets. It is worth noting that, to ensure a fair comparison, all the attack methods including VagueGAN use the same hyperparameters for the effectiveness and stealthiness evaluation experiments in subsections VI-B-a and VI-B-b, respectively, namely $\kappa = 0.2$ and $E = 600$. In other words, the effectiveness of VagueGAN and in subsection VI-B-a and the stealthiness of it in subsection VI-B-b are achieved under the same experimental settings.

a) Effectiveness of Poisoning Attacks: It is evident that the most intuitive measure of the effectiveness of a data poisoning attack is the degree to which the test performance (i.e., task accuracy) of the global model on the main task degrades following the attack. Consequently, the attack effectiveness of data poisoning in this context is characterized by the global model accuracy a_t^p when the attack is present, compared to the no-attack accuracy a_t under the same conditions. For more details, refer to subsection IV-D. With the percentage of malicious clients α ranged from 5% to 30%, the effectiveness of the four attack methods is compared in Table I, and the results are averaged after 10 runs. Compared with the benchmark methods, our VagueGAN mostly achieves better attack effectiveness, though its major advantage is the trade-off

between attack effectiveness and stealthiness. Not surprisingly, increasing the percentage of malicious clients and a non-IID setting lower the global model accuracy. In addition, the attack methods perform differently on different datasets. Compared with Fashion-MNIST and MNIST, CIFAR-10 and CIFAR-100, as well as Mini-ImageNet, are more vulnerable to data poisoning attacks. To explain, we name the rounds in which the number of malicious clients selected by the server is greater than 2 as abnormal rounds, and the rest of the rounds as normal rounds. We find that after any abnormal round, the accuracy rate of the global model generally first decreases, and then returns to normal after a few normal rounds. In comparison, more such normal rounds are needed for CIFAR-10, CIFAR-100, and Mini-ImageNet than for Fashion-MNIST and MNIST. This is because these datasets make the FL task more complex, thereby requiring more normal rounds to recover.

b) Stealthiness of Poisoning Attacks: In this paper, we characterize the stealthiness of a data poisoning attack using statistical distances, such as those obtained between legitimate and poisoned models after applying PCA. This approach is adopted because most existing defenses against data poisoning follow a similar strategy [3], [4], [6], [22]–[25]. They typically obtain low-dimensional model parameters to facilitate subsequent analysis, and use Euclidean distance, cosine similarity, or clustering to measure model differences. This approach can indirectly identify poisoned models without the need for accessing the original data. Take the Fashion-MNIST task under the setting of IID and $\alpha = 20\%$ as an example. After compressing local models to 2-dimensional for visualization using PCA, as shown in Figure 9, the statistical distance between legitimate models (yellow Os for the last 50 rounds) and poisoned models (blue Xs) can be measured. Similarly, the local models can also be visualized in higher dimensions, and our VagueGAN consistently achieves much better attack stealthiness than the benchmark methods.

Second, the attack stealthiness of data poisoning can also be characterized by fluctuations in the global model accuracy a_t^p . Such accuracy fluctuations are linked to attack stealthiness

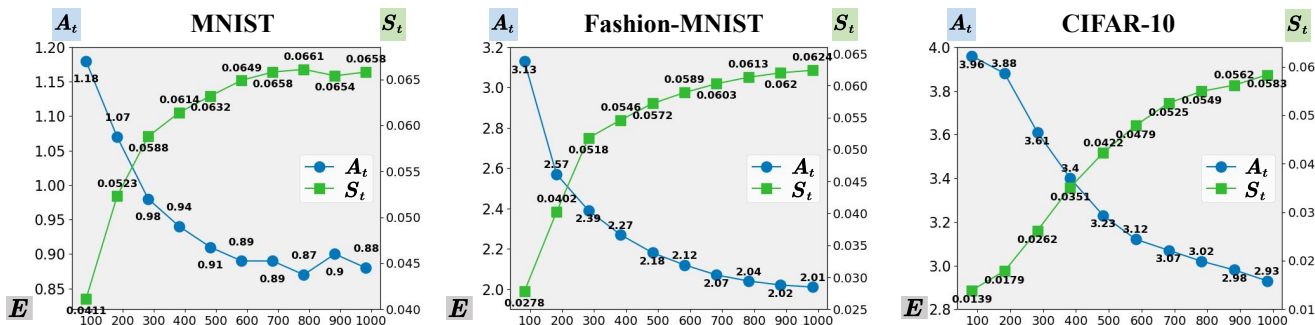


Fig. 12: Impact of VagueGAN training epochs E : A larger E gives higher attack stealthiness but lower attack effectiveness.

TABLE IV: Defense effectiveness of MCD in different attack scenarios with varying proportions of malicious clients.

	M	α	Label flipping	PoisonGAN	Light noise	Heavy noise	SAP noise	VagueGAN
Number of malicious clients	1	5%	1	1	1	1	1	1
detected by	2	10%	2	2	1.9	2	2	2
MCD (average)	4	20%	4	4	3.8	4	3.9	3.9
	6	30%	6	6	5.6	6	5.7	5.8
	a_t	α	Label flipping	PoisonGAN	Light noise	Heavy noise	SAP noise	VagueGAN
Main task test accuracy after MCD deployment (average)(%)	87.97	5%	87.94 (\uparrow 0.21)	87.92 (\uparrow 0.33)	87.97 (\uparrow 0.16)	87.95 (\uparrow 0.24)	87.95 (\uparrow 0.15)	87.94 (\uparrow 0.62)
		10%	87.91 (\uparrow 0.71)	87.92 (\uparrow 0.75)	87.90 (\uparrow 0.32)	87.87 (\uparrow 0.72)	87.89 (\uparrow 0.37)	87.89 (\uparrow 1.11)
		20%	87.88 (\uparrow 1.87)	87.84 (\uparrow 2.07)	87.87 (\uparrow 0.95)	87.83 (\uparrow 1.77)	87.85 (\uparrow 0.86)	87.86 (\uparrow 1.99)
		30%	87.84 (\uparrow 2.36)	87.80 (\uparrow 2.71)	87.86 (\uparrow 1.49)	87.82 (\uparrow 2.26)	87.90 (\uparrow 1.47)	87.89 (\uparrow 3.12)

TABLE V: Defense effectiveness of PCA in different attack scenarios with varying proportions of malicious clients.

	M	α	Label flipping	PoisonGAN	Light noise	Heavy noise	SAP noise	VagueGAN
Number of malicious clients	1	5%	0.9	1	0.6	0.8	0.8	0.1
detected by	2	10%	1.7	1.9	1.4	1.7	1.8	0.2
PCA (average)	4	20%	3.5	3.6	2.7	3.5	3.6	0.6
	6	30%	5.3	5.5	4.2	5.1	5.3	0.9
	a_t	α	Label flipping	PoisonGAN	Light noise	Heavy noise	SAP noise	VagueGAN
Main task test accuracy after PCA deployment (average)(%)	87.97	5%	87.92 (\uparrow 0.19)	87.89 (\uparrow 0.30)	87.93 (\uparrow 0.12)	87.92 (\uparrow 0.21)	87.92 (\uparrow 0.12)	87.34 (\uparrow)
		10%	87.86 (\uparrow 0.66)	87.87 (\uparrow 0.67)	87.79 (\uparrow 0.21)	87.76 (\uparrow 0.61)	87.78 (\uparrow 0.26)	86.79 (\uparrow)
		20%	87.79 (\uparrow 1.78)	87.77 (\uparrow 1.76)	87.71 (\uparrow 0.79)	87.56 (\uparrow 1.50)	87.78 (\uparrow 0.79)	86.01 (\uparrow 0.14)
		30%	87.66 (\uparrow 2.18)	87.61 (\uparrow 2.52)	87.68 (\uparrow 1.31)	87.49 (\uparrow 1.93)	87.82 (\uparrow 1.39)	84.97 (\uparrow 0.20)

TABLE VI: Defense effectiveness of UMAP in different attack scenarios with varying proportions of malicious clients.

	M	α	Label flipping	PoisonGAN	Light noise	Heavy noise	SAP noise	VagueGAN
Number of malicious clients	1	5%	0.7	0.8	0.4	0.8	0.8	0
detected by	2	10%	1.4	1.9	1.2	1.7	1.5	0
UMAP (average)	4	20%	2.9	2.8	1.9	2.3	2.7	0.2
	6	30%	3.3	4.0	2.9	3.7	4.1	0.7
	a_t	α	Label flipping	PoisonGAN	Light noise	Heavy noise	SAP noise	VagueGAN
Main task test accuracy after UMAP deployment (average)(%)	87.97	5%	87.92 (\uparrow 0.19)	87.87 (\uparrow 0.28)	87.93 (\uparrow 0.12)	87.91 (\uparrow 0.20)	87.94 (\uparrow 0.14)	87.34 (\uparrow)
		10%	87.82 (\uparrow 0.62)	87.89 (\uparrow 0.69)	87.79 (\uparrow 0.21)	87.72 (\uparrow 0.57)	87.70 (\uparrow 0.18)	86.79 (\uparrow)
		20%	87.57 (\uparrow 1.56)	87.61 (\uparrow 1.60)	87.59 (\uparrow 0.67)	87.43 (\uparrow 1.37)	87.62 (\uparrow 0.63)	85.96 (\uparrow 0.09)
		30%	87.34 (\uparrow 1.86)	87.39 (\uparrow 2.30)	87.61 (\uparrow 1.24)	87.29 (\uparrow 1.73)	87.60 (\uparrow 1.17)	84.91 (\uparrow 0.14)

because the server’s random selection of clients per round may bring more or less possibly noticeable poisoned models and thus may cause the accuracy fluctuations. Taking the Fashion-MNIST task under the setting of IID and $\alpha = 20\%$ as an example, the accuracy level fluctuating with FL rounds given by VagueGAN versus other data poisoning attack methods is shown in Figure 10. Clearly, our VagueGAN with small accuracy fluctuations mostly approximates the no attack case, but the benchmark methods result in relatively large accuracy fluctuations and are easily detectable even without statistical analysis. Therefore, higher stealthiness of VagueGAN poisoning attack makes it easier to be successful.

C. Performance Trade-off Analysis

As discussed in subsection IV-C, a balanced trade-off between attack effectiveness A_t and stealthiness S_t can be

achieved by setting the values of κ and E appropriately.

a) **Generator Suppression Factor κ** : The value of κ can be adjusted to limit the generation ability of the generator of VagueGAN. Taking the Fashion-MNIST task under the setting of IID, $\alpha = 20\%$, and $E = 400$ as an example, the impact of κ on the trade-off between A_t and S_t is evaluated in Figure 11. It can be seen that increasing κ from 0.1 to 0.4 gives increasing A_t but decreasing S_t . To ensure a not easily detectable attack, a reasonable value of κ , e.g., 0.2, should not be too large.

b) **Number of Training Epochs E** : The value of E can be set to control the fitting state of VagueGAN. When $\alpha = 20\%$, the impact of E on the trade-off between A_t and S_t is evaluated in Figure 12. It can be seen that with the increase of E , effectiveness A_t gradually decreases, while stealthiness S_t gradually increases. The rate of change for both A_t and S_t decreases with the increase of E . On the one hand,

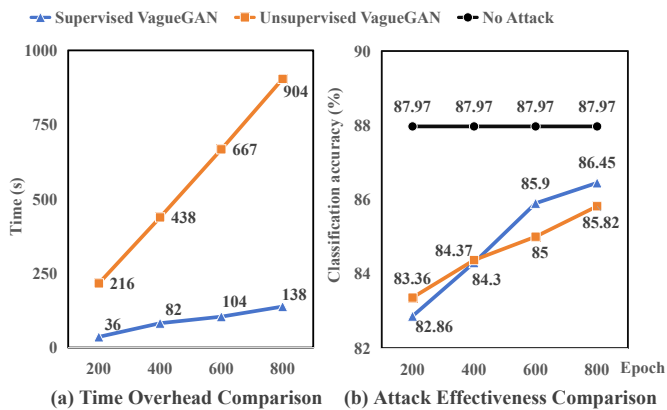


Fig. 13: Supervised vs. unsupervised VagueGAN for time overhead and attack effectiveness: Unsupervised VagueGAN requires higher time overhead but achieves less fluctuant and comparable attacks without label information. the value of E cannot be too small. We find that according to the visualized data poisoning attack will become detectable. Although the performance of A_t is satisfactory at this time, the attack cannot be successful if given a regular defense system. On the other hand, the value of E cannot be too large. For the Fashion-MNIST task as an example, we find that the vague data generated by VagueGAN will be no longer “vague” when $E > 600$ and the quality of vague data will no longer change when $E > 1000$. For this case, the performance of A_t can be overly harmed. More generally, we find that an appropriate value of E can be $0.5e_{lim}$, where e_{lim} is the number of training epochs required for VagueGAN to reach a converged steady state, e.g., $e_{lim} = 600$ for MNIST, 1000 for Fashion-MNIST, and 1600 for CIFAR-10 and CIFAR-100, and 2000 for Mini-ImageNet.

D. Comparison of supervised and unsupervised VagueGANs

In this subsection, we present an experimental comparison of supervised VagueGAN with its unsupervised variant. We evaluate their time overhead, attack effectiveness, and stealthiness with the same settings as follows: generator suppression factor $\kappa=0.2$; the number of training epochs E are taken as 200, 400, 600, and 800, respectively; and the same amount of poisoned data is generated. Firstly, the time overheads are compared for the two VagueGANs on the same experimental device, with a GPU:RTX 3090(24GB) and a CPU:12 vCPU Intel(R) Xeon(R) Platinum 8255C CPU. Figure 13(a) illustrates that the time overhead of unsupervised VagueGAN is greater than that of supervised VagueGAN. Furthermore, the larger the number of training epochs, the greater the discrepancy between the two can be observed. This is due to the necessity that unsupervised VagueGAN maintains an additional classifier, Q , and learns the auxiliary features of the training data.

Secondly, we compare the attack effectiveness of two VagueGANs. Figure 13(b) demonstrates that both VagueGANs exhibit excellent, comparable attack effectiveness. It is noteworthy that the unsupervised attack is more stable and less susceptible to fluctuations in training epochs.

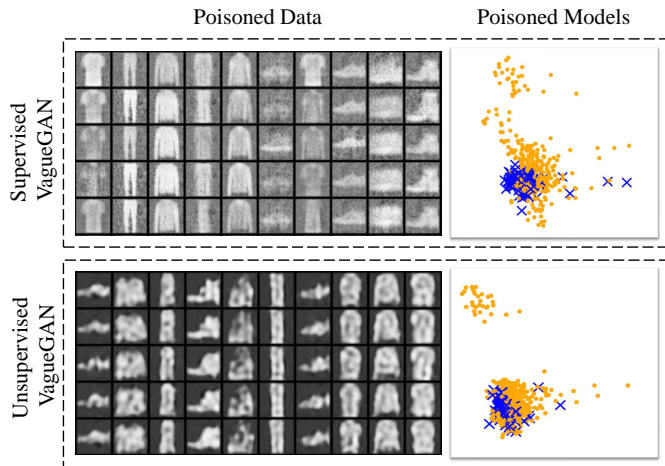


Fig. 14: Supervised vs. unsupervised VagueGAN for attack stealthiness: Both achieve high stealthiness, and poisoned models can look more normal than some legitimate ones.

Finally, we compare the attack stealthiness of the two VagueGANs. As illustrated in Figure 14, the outcomes are compared under the trade-off between effectiveness and stealthiness ($\kappa = 0.2, E = 600$), indicating excellent stealthiness. Furthermore, it is evident that both VagueGANs not only harm the global model performance but also indirectly mislead the distribution of some benign client models and make them look like outliers.

E. Defense Performance Comparison

In this subsection, we evaluate the effectiveness of MCD against different data poisoning attacks in FL, including label flipping attack, label flipping attack with PoisonGAN, noise superimposition attack and VagueGAN. The FL system is set as follows: the total number of clients $N = 20$; the number of clients selected by the server in each round $K = 5$; the number of FL training rounds $T = 200$; the main task dataset is Fashion-MNIST under the setting of IID. We experiment a case where the percentage of malicious clients α is 20%.

a) **Anomaly Detection Capability of MCD:** Tables II and III are the metric tables of MCD in different attack scenarios. Among them, i denotes the client identifier, where red numbers represent malicious clients and green numbers represent the primary benchmark client. $\bar{\theta}_{f,i}^{(2)}$ and $\bar{d}_{f,i}$ are the center and footprint metrics, respectively, used by the MCD for anomaly detection. θ_f^{base} and d_f^{base} serve as the benchmark metrics calculated by the MCD. Light green indicators represent the 100% safe benchmarks ($\hat{\theta}_f^{(2)}, \hat{d}_f$), while light red indicators denote the anomalies detected by the MCD. The anomaly degree for each client, $h_{f,i}$, is computed by the MCD, with red indicating anomalous clients. For detailed definitions of these metrics, please refer to subsection V-B.

Table II present the results of the label flipping attacks and label flipping attacks with PoisonGAN, and ight noise superimposition attack. It is evident from the tables that the $\bar{\theta}_{f,i}^{(2)}$ of the malicious clients exhibit pronounced anomalies in both attack scenarios, and the abnormal behavior of the light noise superimposition attack is similar to that of label flipping

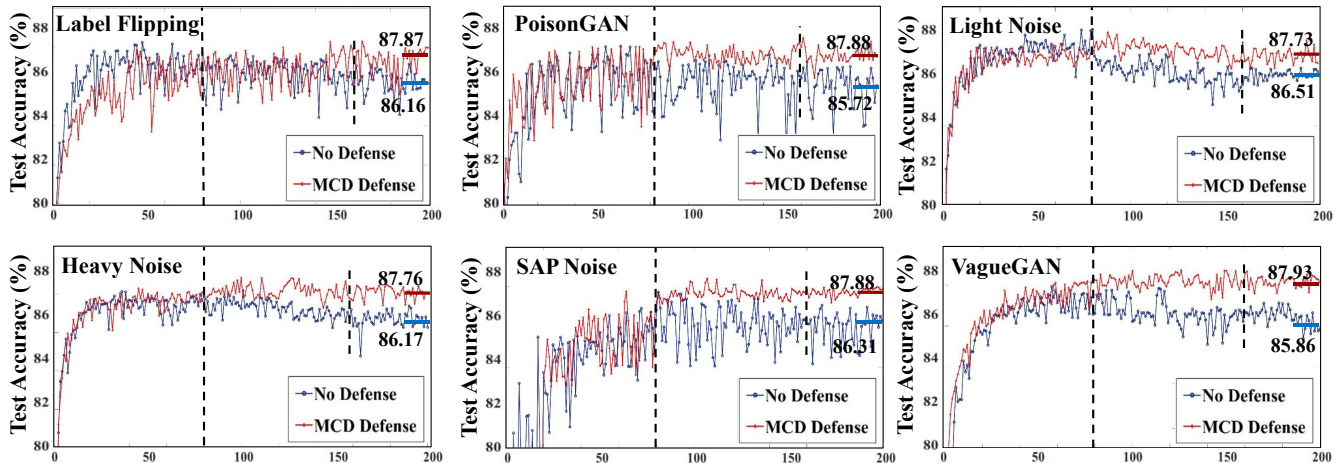


Fig. 15: Defense effectiveness of MCD against different attack methods: Accuracy improvements can be observed when MCD is applied.

attack, as both exhibit anomalies in $\bar{\theta}_{f,i}^{(2)}$. In the scenario of heavy noise and SAP noise superimposition attack as shown in Tables III, the malicious clients demonstrate anomalies in both $\bar{\theta}_{f,i}^{(2)}$ and $\bar{d}_{f,i}$, indicating a poor level of stealthiness.

Table III displays the judgment results of MCD in the data poisoning attack scenario based on VagueGAN. Unlike the previous attacks, the malicious clients in the VagueGAN attack exhibit no anomalies in $\bar{\theta}_{f,i}^{(2)}$. This indicates that the malicious clients taking advantage of GAN have largely learned the distribution of legitimate models and thus are hard to detect if using traditional defense methods like PCA. However, the malicious clients exhibit significantly lower $\bar{d}_{f,i}$ values compared with the normal values of benign clients, meaning that MCD still works for GAN-based attacks like VagueGAN.

b) Overall Defense Effectiveness of MCD: Figure 15 presents the gain in FL performance brought by MCD in six distinct attack scenarios. It is evident that the incorporation of MCD significantly enhances the accuracy of the main task within the FL system. Combining Tables III and IV to Figure 15 and specific experimental observations, we found across all the six attack scenarios, MCD successfully identifies malicious clients during the first inspection and disregards their subsequent updates (as indicated by the long dashed line). To ensure a stable security level for the FL system, MCD performs regular executions in subsequent training rounds (as indicated by the short dashed line).

We further evaluate MCD in attack scenarios with different proportions of malicious clients, as shown in Table IV. The table presents results, on the upper half, for the number of malicious clients detected by MCD, and on the lower half, for the accuracy improvement of the global model brought by MCD. Herein, M (or α) denotes the number (or percentage) of malicious clients within the FL system, and a_t denotes the global model accuracy in the absence of malicious clients. Each scenario is performed 10 times for average results. It is shown that MCD can always identify most of the malicious clients as in the upper half table, and thus achieve a gain in FL performance as in the lower half table.

We also compare MCD with PCA and UMAP, two typical

existing approaches, as shown in Tables V and VI respectively. The results are produced from the same attack scenarios as in Table IV. Each scenario is also performed 10 times for average results. It can be seen that MCD always outperforms PCA and UMAP in terms of the number of malicious clients identified and accuracy improvement, especially under the VagueGAN.

Furthermore, the detection results of four additional defense methods against VagueGAN are evaluated. In Figures 16(a) and 16(b), the cosine similarity results given by CONTRA and the gradient vector angle deviation results given by DnC are presented for the models of three types of client pairs: benign-benign, poisoned-poisoned and benign-poisoned client pairs. The results indicate that the models of the poisoned clients exhibit no significant difference in the deviation statistics of both cosine similarity and vector angle difference distributions do not significantly differ from those of benign clients, indicating that neither CONTRA nor DnC can successfully detect stealthier attacks like VagueGAN. Meanwhile, Figures 16(c) and 16(d) display the results obtained using different clustering methods LoMar and FedDMC, with distinct clusters represented by different colors and malicious clients marked with crosses. Because the feature distribution of poisoned client models is somewhat different from that of benign client models, ideally they can be clustered into different clusters to tell them apart. It can be seen however the clustering results from both LoMar and FedDMC fail to effectively distinguish the malicious and benign client models, indicating that neither LoMar nor FedDMC can successfully detect stealthier attacks like VagueGAN. Therefore, our MCD outperforms these four defense methods in working against GAN-based data poisoning attacks with enhanced attack stealthiness.

As summarized in Table VII, our MCD can effectively work against various data poisoning attacks, especially GAN-based ones like our VagueGAN, and can further contribute to the recovery of FL performance under attacks. It is important to note that this study primarily aims to investigate the impact of poisoned data on FL, so we focus on the case where poisoned data is generated by a consistently applied VagueGAN model.

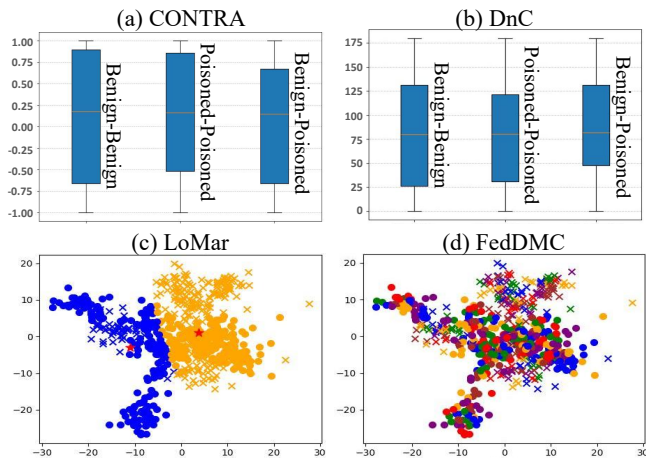


Fig. 16: Detection results of different defenses against VagueGAN: None of them achieves successful detection. Nonetheless, if the attacker were able to adopt a more dynamic version of VagueGAN or integrate it with more sophisticated adaptive attack strategies, the robustness of MCD would be subject to significantly greater challenges.

TABLE VII: Defense methods vs. attack methods: A check mark (or a cross mark) indicates that the defense can (or cannot) counter the corresponding attack.

Defense	Attack						Vague GAN
	Label Flipping	Poison GAN	Light Noise	Heavy Noise	SAP Noise	Cosine Noise	
PCA	✓	✓	×	✓	×	×	×
UMAP	✓	✓	×	×	×	×	×
CONTRA	✓	✓	×	✓	×	×	×
DnC	✓	✓	×	✓	✓	✓	×
Lomar	✓	✓	×	×	×	×	×
FedDMC	✓	✓	×	✓	✓	✓	×
MCD	✓	✓	✓	✓	✓	✓	✓

VII. CONCLUSIONS AND FUTURE WORK

In this paper, we have proposed MCD, a defense countermeasure designed against stealthier data poisoning attacks in FL systems, which reviews local models across multiple feature dimensions. To push the limit of MCD against GAN-based stealthier attacks, we have proposed VagueGAN, a GAN model specifically designed for data poisoning attacks against FL systems. Unlike traditional GANs, our VagueGAN has been verified to generate seemingly legitimate vague data with appropriate amounts of poisonous noise, and thus help strengthen MCD to work against stealthier GAN-based attacks as well as other mainstream ones. Our MCD has been validated to outperform existing defense methods against a range of data poisoning attacks, particularly stealthier GAN-based ones.

In the future, two potential directions are worth pursuing. The first one involves further exploration of more threatening attack methods. In particular, the consistency of GAN outputs has been found to be effective in identifying GAN-poisoned data or models. Hence, a future study can develop more advanced generative models or adaptive attack strategies without such a drawback for improved attack stealthiness. The second one focuses on exploring effective and universally applicable defense mechanisms. Although our MCD has been validated to be useful against GAN-based attacks, the model consistency it relies on may not hold if the attacks are implemented

in varying settings, such as those involving adaptive attack strategies. Hence, a future study can produce better adaptive AI-driven techniques for enhanced defense capabilities.

REFERENCES

- [1] W. Wei and L. Liu, "Trustworthy distributed ai systems: Robustness, privacy, and governance," *ACM Comput Surv*, 2024.
- [2] N. Rodríguez-Barroso, D. Jiménez-López, M. V. Luzón, F. Herrera, and E. Martínez-Cámara, "Survey on federated learning threats: concepts, taxonomy on attacks and defences, experimental study and challenges," *Inf. Fusion*, vol. 90, pp. 148–173, 2023.
- [3] V. Tolpegin, S. Truex, M. E. Gurosy, and L. Liu, "Data poisoning attacks against federated learning systems," in *Proc. ESORICS*, 2020, pp. 480–501.
- [4] D. Upreti, H. Kim, E. Yang, and C. Seo, "Defending against label-flipping attacks in federated learning systems using uniform manifold approximation and projection," *IAES International Journal of Artificial Intelligence (IJ-AI)*, vol. 13, no. 1, pp. 459–466, 2024.
- [5] S. Shen, S. Tople, and P. Saxena, "Auror: Defending against poisoning attacks in collaborative deep learning systems," in *Proc. ACM ACSAC*, 2016, pp. 508–519.
- [6] X. Li, Z. Qu, S. Zhao, B. Tang, Z. Lu, and Y. Liu, "Lomar: A local defense against poisoning attack on federated learning," *IEEE Trans. Dependable Secure Comput*, 2021.
- [7] H. S. Sikandar, H. Waheed, S. Tahir, S. U. Malik, and W. Rafique, "A detailed survey on federated learning attacks and defenses," *Electronics*, vol. 12, no. 2, p. 260, 2023.
- [8] X. Zhang, J. Zhang, K.-H. Chow, J. Chen, Y. Mao, M. Rahouti, X. Li, Y. Liu, and W. Wei, "Visualizing the shadows: Unveiling data poisoning behaviors in federated learning," in *Proc. ICDCS*. IEEE, 2024, pp. 1431–1434.
- [9] L. Lyu, H. Yu, and Q. Yang, "Threats to federated learning: A survey," *arXiv preprint arXiv:2003.02133*, 2020.
- [10] R. Gosselin, L. Vieu, F. Loukil, and A. Benoit, "Privacy and security in federated learning: A survey," *Appl. Sci*, vol. 12, no. 19, p. 9901, 2022.
- [11] V. Mothukuri, R. M. Parizi, S. Pouriyeh, Y. Huang, A. Dehghantanha, and G. Srivastava, "A survey on security and privacy of federated learning," *Future Gener. Comput. Syst*, vol. 115, pp. 619–640, 2021.
- [12] M. S. Jere, T. Farnan, and F. Koushanfar, "A taxonomy of attacks on federated learning," *IEEE S&P*, vol. 19, no. 2, pp. 20–28, 2020.
- [13] G. Xia, J. Chen, C. Yu, and J. Ma, "Poisoning attacks in federated learning: A survey," *IEEE Access*, vol. 11, pp. 10 708–10 722, 2023.
- [14] J. Zhang, B. Chen, X. Cheng, H. T. T. Binh, and S. Yu, "Poisoning: Generative poisoning attacks against federated learning in edge computing systems," *IEEE Internet Things J*, vol. 8, no. 5, pp. 3310–3322, 2020.
- [15] J. Zhang, J. Chen, D. Wu, B. Chen, and S. Yu, "Poisoning attack in federated learning using generative adversarial nets," in *Proc. IEEE TrustCom/BigDataSE*, 2019, pp. 374–380.
- [16] D. Cao, S. Chang, Z. Lin, G. Liu, and D. Sun, "Understanding distributed poisoning attack in federated learning," in *Proc. IEEE ICPADS*, 2019, pp. 233–239.
- [17] I. Goodfellow, J. Pouget-Abadie, M. Mirza, B. Xu, D. Warde-Farley, S. Ozair, A. Courville, and Y. Bengio, "Generative adversarial networks," *Commun. ACM*, vol. 63, no. 11, pp. 139–144, 2020.
- [18] B. Hitaj, G. Ateniese, and F. Perez-Cruz, "Deep models under the gan: information leakage from collaborative deep learning," in *Proc. ACM CCS*, 2017, pp. 603–618.
- [19] Y. Shi, T. Erpek, Y. E. Sagduyu, and J. H. Li, "Spectrum data poisoning with adversarial deep learning," in *Proc. IEEE MILCOM*, 2018, pp. 407–412.
- [20] H. Huang, J. Mu, N. Z. Gong, Q. Li, B. Liu, and M. Xu, "Data poisoning attacks to deep learning based recommender systems," in *Proc. NDSS*. Internet Society, 2021.
- [21] X. Zhang, X. Zhu, and L. Lessard, "Online data poisoning attacks," in *Proc. LADC*, 2020, pp. 201–210.
- [22] V. Shejwalkar and A. Houmansadr, "Manipulating the byzantine: Optimizing model poisoning attacks and defenses for federated learning," in *Proc. NDSS*, 2021.
- [23] Z. Zhang, X. Cao, J. Jia, and N. Z. Gong, "Fldetector: Defending federated learning against model poisoning attacks via detecting malicious clients," in *Proc. ACM KDD*, 2022, pp. 2545–2555.
- [24] X. Shen, Y. Liu, F. Li, and C. Li, "Privacy-preserving federated learning against label-flipping attacks on non-iid data," *IEEE Internet Things J*, 2023.

- [25] S. Awan, B. Luo, and F. Li, "Contra: Defending against poisoning attacks in federated learning," in *Proc. ESORICS 2021, Part I 26*, 2021, pp. 455–475.
- [26] X. Mu, K. Cheng, Y. Shen, X. Li, Z. Chang, T. Zhang, and X. Ma, "Feddmc: Efficient and robust federated learning via detecting malicious clients," *IEEE Trans. Dependable Secure Comput.*, vol. 21, no. 6, pp. 5259–5274, 2024.
- [27] Y. Wang, T. Zhu, W. Chang, S. Shen, and W. Ren, "Model poisoning defense on federated learning: A validation based approach," in *Proc. NSS*, 2020, pp. 207–223.
- [28] X. Cao, J. Jia, and N. Z. Gong, "Provably secure federated learning against malicious clients," in *Proc. AAAI*, 2021.
- [29] Y. Zhao, J. Chen, J. Zhang, D. Wu, M. Blumenstein, and S. Yu, "Detecting and mitigating poisoning attacks in federated learning using generative adversarial networks," *Concurrency Comput. Pract. Exper.*, vol. 34, no. 7, p. e5906, 2022.
- [30] S. Li, Y. Cheng, Y. Liu, W. Wang, and T. Chen, "Abnormal client behavior detection in federated learning," *arXiv preprint arXiv:1910.09933*, 2019.
- [31] Y. Jiang, W. Zhang, and Y. Chen, "Data quality detection mechanism against label flipping attacks in federated learning," *IEEE Trans. Inf. Forensics Security*, vol. 18, pp. 1625–1637, 2023.
- [32] P. R. Ovi, A. Gangopadhyay, R. F. Erbacher, and C. Busart, "Confident federated learning to tackle label flipped data poisoning attacks," in *Proc. SPIE 12538, Artificial Intelligence and Machine Learning for Multi-Domain Operations Applications V*, 2023.
- [33] Y.-C. Lai, J.-Y. Lin, Y.-D. Lin, R.-H. Hwang, P.-C. Lin, H.-K. Wu, and C.-K. Chen, "Two-phase defense against poisoning attacks on federated learning-based intrusion detection," *Comput. Secur.*, vol. 129, p. 103205, 2023.
- [34] J. Yang, J. Zheng, T. Baker, S. Tang, Y.-a. Tan, and Q. Zhang, "Clean-label poisoning attacks on federated learning for iot," *Expert Syst.*, vol. 40, no. 5, p. e13161, 2023.
- [35] O. Marfoq, G. Neglia, A. Bellet, L. Kameni, and R. Vidal, "Federated multi-task learning under a mixture of distributions," *Adv. Neural Inf. Process. Syst.*, vol. 34, pp. 15 434–15 447, 2021.
- [36] D. Gragnaniello, F. Marra, G. Poggi, and L. Verdoliva, "Analysis of adversarial attacks against cnn-based image forgery detectors," in *Proc. EUSIPCO*. IEEE, 2018, pp. 967–971.
- [37] X. Chen, C. Liu, B. Li, K. Lu, and D. Song, "Targeted backdoor attacks on deep learning systems using data poisoning," *arXiv preprint arXiv:1712.05526*, 2017.